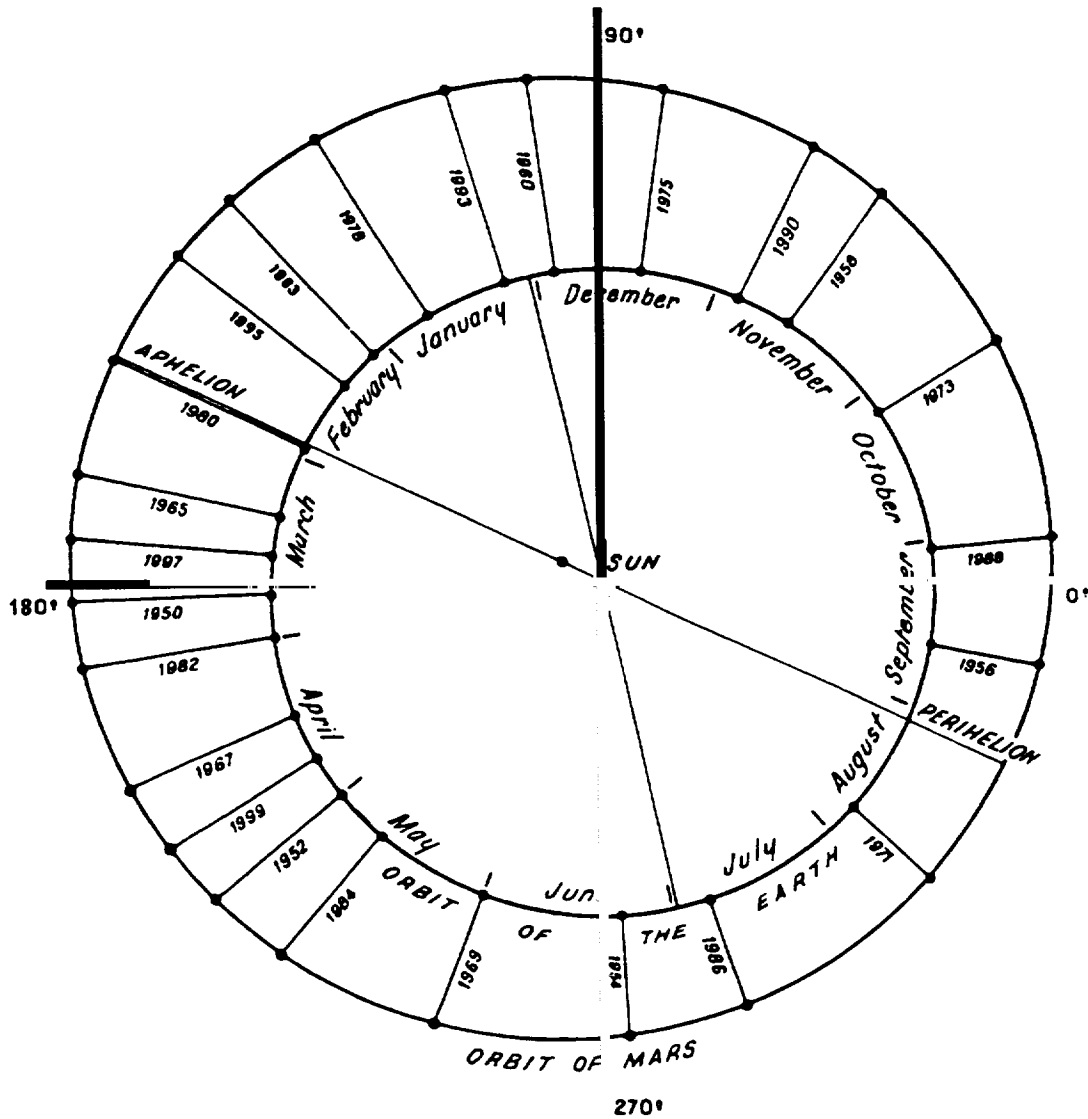


WORKSHOP ON MARS TELESCOPIC OBSERVATIONS



LPI Technical Report Number 95-04

Lunar and Planetary Institute 3600 Bay Area Boulevard Houston TX 77058-1113
LPI/TR-95-04

**WORKSHOP ON
MARS TELESCOPIC OBSERVATIONS**

Edited by

J. F. Bell III and J. E. Moersch

Held at
Cornell University, Ithaca, New York

August 14–15, 1995

Sponsored by
Lunar and Planetary Institute

Lunar and Planetary Institute 3600 Bay Area Boulevard Houston TX 77058-1113

LPI Technical Report Number 95-04
LPI/TR--95-04

Compiled in 1995 by
LUNAR AND PLANETARY INSTITUTE

The Institute is operated by the Universities Space Research Association under Contract No. NASW-4574 with the National Aeronautics and Space Administration.

Material in this volume may be copied without restraint for library, abstract service, education, or personal research purposes; however, republication of any paper or portion thereof requires the written permission of the authors as well as the appropriate acknowledgment of this publication.

This report may be cited as

Bell J. F. III and Moersch J. E., eds. (1995) *Workshop on Mars Telescopic Observations*. LPI Tech. Rpt. 95-04, Lunar and Planetary Institute, Houston. 33 pp.

This report is distributed by

ORDER DEPARTMENT
Lunar and Planetary Institute
3600 Bay Area Boulevard
Houston TX 77058-1113

Mail order requestors will be invoiced for the cost of shipping and handling.

Cover: Orbits of Mars (outer ellipse) and Earth (inner ellipse) showing oppositions of the planet from 1954 to 1999. From C. Flammarion (1954) *The Flammarion Book of Astronomy*, Simon and Schuster, New York.

Introduction

The Mars Telescopic Observations Workshop, held August 14–15, 1995, at Cornell University in Ithaca, New York, was organized and planned with two primary goals in mind: The first goal was to facilitate discussions among and between amateur and professional observers and to create a workshop environment fostering collaborations and comparisons within the Mars observing community. The second goal was to explore the role of continuing telescopic observations of Mars in the upcoming era of increased spacecraft exploration.

Initial announcements for the workshop were sent out to all members of the Mars Surface and Atmosphere Through Time (MSATT) study group, to many other telescopic observers on the LPI mailing list, to a number of amateur observing groups, and to several popular astronomy and planetary science magazines. The 24 papers presented at the workshop described the current NASA plans for Mars exploration over the next decade, current and recent Mars research being performed by professional astronomers, and current and past Mars observations being performed by amateur observers and observing associations. The workshop was divided into short topical sessions concentrating on programmatic overviews, groundbased support of upcoming spacecraft experiments, atmospheric observations, surface observations, modeling and numerical studies, and contributions from amateur astronomers.

The workshop, which summarized the present state of knowledge on a number of issues and was attended by many of the currently active professional Mars telescopic observers, generated spirited discussions among the participants, particularly when the potential interactions between amateur and professional observers were identified throughout the meeting.

Program

Monday, August 14, 1995

8:00 a.m.–9:00 a.m. Registration

9:00 a.m.–9:30 a.m. *Welcome and Introduction*
 J. Bell, Cornell University
 J. Moersch, Cornell University

9:30 a.m.–10:30 a.m.

NASA PLANETARY ASTRONOMY AND MARS PROGRAM OVERVIEWS

Planetary Astronomy Program Roadmap
 E. Barker, NASA Headquarters, Planetary Astronomy Program

Mars Surveyor Program Ground-based Observing
 S. Squyres, Cornell University, Chair, NASA Mars Science Working Group

11:00 a.m.–12:30 p.m.

OBSERVATIONS: ATMOSPHERE I

High Resolution Spectroscopic Measurements of Atmospheric Water Vapor
 A. Sprague, University of Arizona

Photometric Modeling of Dust and Cloud Opacities
 K. Herkenhoff, Jet Propulsion Laboratory

“Mars Watch” Observations from the Lowell Observatory
 L. Martin, Lowell Observatory

2:00 p.m.–5:00 p.m.

OBSERVATIONS: ATMOSPHERE II

HST Observations and Spectroscopic Observations from Ritter Observatory
 P. James, University of Toledo

HST Observations of Atmospheric Dust and Ice Abundances
 D. Crisp, Jet Propulsion Laboratory (presentation given by J. Bell)

Millimeter Observations of Hydrogenous and Organic Compounds
 D. Moreau, Belgian Institute for Space Aeronomy, Belgium

Near Infrared Imaging Spectroscopy of Clouds and Volatiles

D. Klassen, University of Wyoming

Photographic Observations of the North Polar Hood

T. Akabane, Kyoto University, Japan

5:00 p.m.–6:30 p.m. Special Discussion and Reception, Terrace Lounge, Statler Hotel

Tuesday, August 15, 1995

8:30 a.m.–10:00 a.m.

OBSERVATIONS: ATMOSPHERIC ISOTOPES

Atmospheric Water Vapor on Mars: A Search for Enrichment of HDO/H₂O

M. Disanti, NASA Goddard Space Flight Center

High-Resolution Spectroscopy of Mars at 3.7 and 8 μ m: Hydrogen, Oxygen, and Carbon Isotope Ratios and Implications for Evolution

V. A. Kransnopolsky, NASA Goddard Space Flight Center

**CONTRIBUTIONS FROM THE ASSOCIATION OF LUNAR
AND PLANETARY OBSERVERS**

Telescopic Observations of Mars: 1994–1995 Apparition

D. Parker, Coral Gables, Florida

10:30 a.m.–11:30 a.m.

Meteorological Survey of Mars for Opposition Years 1965–1995

J. Beish, Miami, Florida (presentation given by D. Parker)

Summary of 1992–1995 A.L.P.O. Mars Observations

D. Troiani, Schaumburg, Illinois (presentation given by D. Joyce)

11:30 a.m.–12:30 p.m.

MODELING AND NUMERICAL STUDIES

Chemistry, Stability, and Evolution of the Martian Atmosphere

S. Atreya, University of Michigan

Storm Zones on Mars

J. Hollingsworth, NASA Ames Research Center

1:30 p.m.–3:30 p.m.

OBSERVATIONS: SURFACE

Thermal Infrared Observations from KAO, IRTF, and WIRO

T. Roush, NASA Ames Research Center

Thermal Infrared Observations from Palomar During the 1995 Opposition

J. Moersch, Cornell University

HST Observations of Time-Variable Surface Features

S. Lee, University of Colorado

Near Infrared Imaging Spectroscopy from the IRTF During the 1990–1995 Oppositions

J. Bell, Cornell University

4:00 p.m.–5:30 p.m.

GROUND-BASED SUPPORT OF UPCOMING SPACECRAFT EXPERIMENTS

Mars Pathfinder Mission

M. Golombek, Jet Propulsion Laboratory (presentation given by K. Herkenhoff)

Mars Global Surveyor Camera

P. Thomas, Cornell University

Mars Global Surveyor Thermal Emission Spectrometer

K. Edgett, Arizona State University

Contents

Statement of Consensus	1
Summary of Technical Sessions	3
Abstracts	
Morphological Features and Opacities of the Martian North Polar Hood <i>T. Akabane, K. Iwasaki, and L. J. Martin</i>	9
Mars Atmosphere: Chemistry, Stability, and Evolution <i>S. K. Atreya</i>	9
Near-Infrared Imaging Spectroscopy of Mars from the IRTF in 1994 and 1995 <i>J. F. Bell III, W. F. Golisch, D. M. Griep, C. D. Kaminski, and T. L. Roush</i>	10
WFPC2 Observations of Mars <i>D. Crisp, J. F. Bell III, and the WFPC Science Team</i>	11
Atmospheric Water Vapor on Mars: A Search for Enrichment of HDO/H ₂ O in the North Polar Cap <i>M. A. DiSanti and M. J. Mumma</i>	11
Synergy Between Telescopic Observations of Mars from Earth and the Mars Global Surveyor Thermal Emission Spectrometer <i>K. S. Edgett, T. L. Roush, R. T. Clancy, and P. R. Christensen</i>	12
Mars Pathfinder Mission, Science Investigations, and Telescopic Observational Support <i>M. P. Golombek and K. E. Herkenhoff</i>	14
Telescopic Determination of Martian Atmospheric Opacity <i>K. E. Herkenhoff and J. Hillier</i>	14
Winter Storm Zones on Mars <i>J. L. Hollingsworth, R. M. Haberle, A. F. C. Bridger, and J. Schaeffer</i>	15
Hubble Space Telescope Observations of Mars: 1994–1995 <i>P. B. James, J. F. Bell III, R. T. Clancy, S. W. Lee, L. J. Martin, and M. J. Wolff</i>	16
Near-Infrared Imaging Spectroscopy of Clouds and Volatiles <i>D. R. Klassen, J. F. Bell III, and R. R. Howell</i>	17

High-Resolution Spectroscopy of Mars at 3.7 and 8 μm : Hydrogen, Oxygen, and Carbon Isotope Ratios and Implications for Evolution <i>V. A. Krasnopolsky, M. J. Mumma, and G. L. Bjoraker</i>	18
HST Observations of Time-Variable Albedo Features on Mars <i>S. W. Lee, M. J. Wolff, P. B. James, L. J. Martin, R. T. Clancy, and J. F. Bell III</i>	19
“Mars Watch” Observations from the Lowell Observatory, and Observed Cloudiness in 1994–1995: Possible Implications for Dust Activity <i>L. J. Martin, J. F. Bell III, P. B. James, S. W. Lee, and D. Thompson</i>	19
Millimeter and Infrared Observations of Hydrogenous and Organic Compounds on Mars <i>D. Moreau, A. Marten, J. Rosenqvist, Y. Biraud, and C. Muller</i>	20
Thermal Infrared Observations of Mars During the 1995 Opposition <i>J. Moersch, T. Hayward, P. Nicholson, S. Squyres, and J. Van Cleve</i>	21
Telescopic Observations of Mars: 1994–1995 Apparition <i>D. C. Parker and J. D. Beish</i>	22
Thermal Infrared Spectra of Mars Obtained in 1988, 1990, and 1993 <i>T. L. Roush, G. C. Sloan, J. F. Bell III, and C. W. Rowland</i>	23
Spectroscopic Measurements of Atmospheric Water Vapor <i>A. Sprague, D. Hunten, and R. Hill</i>	24
Mars Global Surveyor Camera: Context of Earth-based Observations <i>P. Thomas</i>	24
The 1992–1993 Apparitions of Mars <i>D. M. Troiani</i>	25
1994–1995 Apparition of Mars <i>D. M. Troiani</i>	27
Prospects for Observing Mars from Antarctica During the Upcoming Oppositions of 1999, 2001, and 2003 <i>F. R. West</i>	29
List of Workshop Participants	31

Statement of Consensus

With the beginning of the decade-long Mars Surveyor program close at hand, our understanding of Mars is about to increase dramatically. As participants in the Mars Telescopic Observations Workshop, held at Cornell University in August 1995, and as representatives of the Mars observing community as a whole, we feel that it is important to identify the most effective roles that Earth-based (e.g., groundbased telescopic, HST, ISO) observations of Mars can play during this historic period of exploration. While the primary focus of Mars Surveyor will be spacecraft-based science, the results of the workshop suggest several niches in which Earth-based observations can complement and extend the planned suite of spacecraft observations. These fall into three broad categories, summarized in Table 1 and detailed below.

TABLE 1. Specific areas for continued groundbased studies of Mars.

Mission-Specific Support Observations

- ❖ Are there dust storms at the landing sites that could affect available lander power?
- ❖ What is the atmospheric state (temperature, dust opacity, cloud cover) prior to the mission?
- ❖ How do local lander temperature and dust and cloud opacity during the mission compare to global values?

Global-Scale Monitoring

- ❖ Cover local times that will not be covered by a polar orbiter (early morning, late afternoon)
- ❖ Assess diurnal variations across large geographic areas for comparisons with variations observed at landing sites

Spectral Coverage and Resolution

- ❖ Obtain data at diagnostic wavelengths not measured by spacecraft instruments
 - ❖ Obtain data at higher spectral resolution than spacecraft instruments in order to provide better constraints on mineralogy, atmospheric composition
-

MISSION-SPECIFIC SUPPORT OBSERVATIONS

Earth-based observations of Mars will play critical mission support roles for Mars Surveyor spacecraft. The first example of this will occur in 1997 during the cruise phase of the Mars Pathfinder mission, when Earth-based images of Pathfinder's primary landing site are needed to determine atmospheric temperature and dust activity for mission safety and planning. Subsequent Earth-based observations during the primary mission will be used to place local temperature and opacity measurements from the lander into a regional and global context. Later missions are likely to require similar

types of support observations, as well as high-spatial-resolution data obtained during possible gaps between missions. Such observations will substantially enhance the scientific value of data returned from Mars missions.

GLOBAL-SCALE MONITORING

One of the strengths of the planned suite of spacecraft in the Mars Surveyor program is that they will study the planet at higher spatial resolution than ever before. However, Mars is very dynamic on a global scale, and Earth-based synoptic observations of the planet will be important in the interpretation of more localized spacecraft data. For example, the Mars Global Surveyor (MGS) orbiter will be able to image the surface at resolutions up to 1.5 m, but because of the spacecraft's Sun-synchronous orbit, the local times of these observations will be restricted to a narrow range around 2 a.m./p.m. for most of the planet except the highest latitudes. This geometry will preclude MGS from making dynamic observations of many diurnal features known to appear on Mars, such as the morning and evening atmospheric hazes and ground frosts. Earth-based full-disk imaging of Mars will complement MGS observations much in the same way that GOES full-disk imaging complements the polar-orbiting NOAA satellite data for weather forecasting here on Earth. The importance of global observations concurrent with spacecraft-based Sun-synchronous data is not limited to visible wavelength imaging. For example, surface properties such as thermal inertia are most easily measured when data are available from a wide range of local times.

The amateur Mars observing community is particularly well-positioned to aid in visible wavelength global monitoring. A network of highly skilled amateurs is already in place, and they are unique in their ability to collect Mars images frequently and long before and after opposition, in contrast to professional observers who are usually able to observe only a handful of times per year. This is important because the value and effectiveness of visible wavelength observations are greatly enhanced when the planet is monitored on a near-continuous basis. Earth-based and spacecraft-based observers alike will do well to foster increased links to this valuable source of experience and data. Additionally, interaction between amateur and professional observers serves to further NASA's educational mission.

SPECTRAL COVERAGE AND RESOLUTION

While Mars Surveyor spacecraft will study Mars in many regions of the spectrum in great detail, there are some notable gaps in this coverage that can be filled with Earth-based observations. There are currently no plans in the Surveyor

program for instruments that would study Mars at ultraviolet, near-infrared, or radio wavelengths, and planned narrow-band spectral coverage in the visible region is limited. No plans exist for high-spectral-resolution spacecraft observations of atmospheric water vapor, isotopes, or other trace species such as O₃, CO, O₂, and H₂O₂. Past experience has shown that observations spanning a wide range of spectral regions offer important constraints on atmospheric and/or surface composition. It is likely that further Earth-based study in spectral regions and/or at spectral resolutions not observed by Mars Surveyor instruments will continue to yield new, unique, and complementary results.

SUMMARY

These are the primary areas in which we believe Earth-based observations can best contribute to Mars science over the next decade. As a community, we are excited and encouraged by NASA's plans for continued, intensive exploration of Mars and we look forward to contributing in the ways in which we are uniquely capable.

—*Participants of the Mars Telescopic
Observations Workshop*

Summary of Technical Sessions

OVERVIEWS

Participants at the workshop heard programmatic overview talks by Ed Barker, NASA Headquarters Planetary Astronomy Program Discipline Scientist, and Steve Squyres, chair of the NASA Mars Science Working Group. Barker's presentation concentrated on the future of the planetary exploration program after the current radical changes in NASA have been implemented. While nothing is certain during these times of fiscal restraint and cutbacks, it was reassuring for many participants to hear that core research programs, such as the NASA Planetary Astronomy program that supports most U.S. professional Mars observing programs, are being spared major cuts in funding in the current reorganizational scheme. At the same time, there was some concern expressed by participants that plans to possibly eliminate the current scheme of "fixed" percentages of planetary observing time on major facilities like IRTF and HST could lead to a substantial decrease in the ability to conduct long-term Mars observational programs or to conduct detailed Mars observations requiring instruments or capabilities only available on these national facility telescopes. Barker assured workshop participants that he and others at NASA HQ understand these concerns and are doing all they can to fund the best possible science within a base of ever-shrinking resources.

The overview presentation by Squyres outlined the primary goals of the upcoming decade-long Mars Surveyor program. He pointed out that Mars research, unlike most other NASA and federally funded science programs, is currently enjoying wide popular and congressional support. The primary goals of the Mars Surveyor program can be grouped under the categories life, climate, and resources, with the common thread being the role of water on Mars. NASA plans to send two launches to Mars at each launch opportunity, starting in 1996 with the Pathfinder lander and the Mars Global Surveyor orbiter. Future plans are still evolving, but the 1998 and 2001 launches would each include another orbiter and lander, the 2003 launches may include an ESA orbiter and a series of microlanders in a global network, and by 2005 it may be possible to consider some sort of sample return missions. Squyres identified two major gaps in the Mars Surveyor program that can be filled by groundbased and Earth-orbital observations: The first gap is wavelength coverage, as there are no plans for near-IR or UV spectral coverage by any of the Mars Surveyor instruments, and the visible-wavelength sampling is rather coarse and could be supplemented by higher-spectral-resolution data. The second gap is temporal coverage, as all planned Mars Surveyor orbits are low and Sun-synchronous, passing over most surface regions at either 2 a.m. or 2 p.m. only. Thus, morning or late afternoon coverage cannot be obtained from the mapping orbits.

GROUND BASED SUPPORT OF MARS SPACECRAFT EXPERIMENTS

Participants received additional details on the need for telescopic support of planned spacecraft investigations from representatives of the Mars Pathfinder lander and Mars Global Surveyor orbiter camera and spectrometer science teams. For Pathfinder, it will be critical to obtain determinations of the dust opacity history during the cruise phase of the mission, which coincides with the spring 1997 Mars opposition, as well as during the primary mission, which begins in July 1997 [1]. These observations will help to constrain the lander's power budget and operating scenario, as the presence of dust severely influences the amount of power (sunlight) available to the instruments. Also, Earth-based observations of the dust opacity and variability of other atmospheric phenomena will help to place the Pathfinder data, obtained from one site near 19.5°N, 32.8°W, into a global context. For the Mars Orbiter Camera (MOC), the most important telescopic contributions will be obtaining morning and late-afternoon observations of regions imaged by MOC at high resolution at 2 p.m. local time, and obtaining additional spectral coverage (more channels, near-IR and UV coverage) to assist with the mineralogic interpretation of the two-color MOC data [2]. For the Mars Orbiter Thermal Emission Spectrometer (TES), the most important telescopic contributions will be in the measurement of surface physical properties (from radar or morning/evening thermal-IR observations), dust opacity and atmospheric temperature variations (from visible or microwave observations), and surface mineralogy (from visible and near-IR observations) that can be used to assist with and extend the interpretation of the TES spectra obtained from orbit [3].

ATMOSPHERIC OBSERVATIONS

Groundbased observations of the martian atmosphere using a wide variety of techniques from the UV through millimeter wavelengths continue to produce important new results. Synoptic observations of water vapor using high-resolution spectroscopy [4] are being used to determine whether seasonal and/or interannual differences in the behavior of water vapor have occurred since the Viking MAWD observations in the late 1970s. New measurement techniques allow for latitudinal resolution in the groundbased data, facilitating comparisons with the high-spatial-resolution MAWD data. Large interannual and latitudinal variations in water vapor are seen in the data, and many of the variations reported by [4] are consistent with the behavior of water vapor during the Viking years. There was general agreement among participants, based also on the amateur observations discussed below, that the very high water vapor abundances observed in 1969 by Barker and others represents a possibly real anomaly

that warrants further investigation at higher spatial resolution during the same season in future apparitions. Additional attempts at spatially resolving atmospheric water vapor and (especially) HDO variations [5] also rely on high-resolution spectroscopy. Preliminary observations during 1993 yielded tantalizing but as-yet inconclusive results on the distribution of HDO; attempts at confirmation of these results during the 1995 apparition were foiled by bad weather at the IRTF. Plans are being formulated to attempt the HDO observations again during 1997, using even better instrumentation. An obvious region of collaboration was identified between the Arizona group pursuing the H₂O observations and the NASA Goddard group pursuing the HDO observations.

Additional isotopic observations are concentrating on refining the rather poorly constrained values of ¹⁸O/¹⁷O and ¹³C/¹²C, as well as confirming and further refining the martian D/H ratio [6]. These high-spectral-resolution observations are also being used to constrain the abundances of trace species like CH₄, H₂O₂, H₂CO, and HCl in the martian atmosphere. The preliminary results reported at the workshop have important implications for the early evolution of the martian atmosphere, particularly regarding impact erosion. However, discrepancies with some of the Viking atmospheric measurements remain unexplained and warrant further investigation. Other observations at millimeter wavelengths are also providing constraints on the abundances of trace atmospheric species [7]. These observations, conducted between 1992 and 1995, searched for millimeter spectral lines arising from H₂CO, H₂O₂, HO₂, and CH₃OH. Much of the interpretive effort thus far has concentrated on the formaldehyde observations, in an attempt to confirm the high formaldehyde observations reported by the Phobos 2 spacecraft measurements in 1988–1989. While the observations of [7] agree with the infrared observations of [6] and indicate H₂CO abundances up to 3 orders of magnitude lower than the Phobos 2 measurements, the possibility of an error in the Phobos 2 data was discounted by [7] in favor of the possibility that some sort of local heterogeneous catalytic process, possibly involving airborne dust, may act to increase the concentration of organic molecules in the atmosphere. Many participants expressed skepticism at this possibility, but all agreed that the potential discrepancy deserves further additional study.

Groundbased telescopic imaging studies of atmospheric phenomena are also producing new and exciting results. Visible to near-IR images and photographs reveal extensive, though not unprecedented, cloudiness on Mars during northern spring [8–10]. There was much discussion among workshop participants about whether the increased cloudiness is necessarily correlated with a decrease in atmospheric dust opacity and dust storm activity. Experience before and during the Viking years showed that condensate clouds may play a role in the formation of dust storms, providing a source of turbulence for dust raising [8]. Some participants speculated

that the current period of high cloudiness and low dust opacity may not persist because of this possible feedback between condensates and dust. New techniques are being developed for deriving the opacities of condensate clouds [9] and atmospheric dust [11] using well-calibrated imaging data. These techniques rely on radiative transfer modeling of relative and absolute flux values from different regions of the planet, concentrating especially on the limbs where the greatest atmospheric pathlength is encountered. The routine ability to determine atmospheric dust opacity from quantitative CCD observations using computationally efficient and geometrically rigorous algorithms [11] is needed in order to monitor the evolution of atmospheric dust on diurnal, seasonal, and interannual timescales. As discussed above, this information is critical for planning of Pathfinder Lander mission operations [1], as well as for scheduling and planning of infrared spectroscopic observations of Mars to be obtained from the ESA Infrared Space Observatory (ISO) satellite in 1996–1997 [7].

The opacity of the north polar hood (NPH) clouds has been estimated to be around 0.6 based on observations in 1969, 1986, and 1990 [9]. In order for the fact that the hood is not visible in the red to be consistent with this rather low opacity value, the mean particle size of polar hood materials must be very small, probably comparable in size to the wavelength of blue light. Near-infrared imaging spectroscopic observations provide a way not only of mapping clouds and surface volatiles, but of uniquely determining their composition as well. For example, water ice clouds can be discriminated from CO₂ ice clouds based on the presence of specific absorption features in the 3.0- to 3.6- μ m region [10,12]. The ability to map these absorption features and place their distribution into a global context along with topography, albedo, geology, etc., is a particularly strong point. Observations from 1990 through 1995 have revealed the extensive H₂O ice polar hood clouds as well as evidence for spatially confined polar CO₂ ice clouds [10].

Finally, observations of the martian atmosphere using the Hubble Space Telescope (HST) have produced unique and exciting results during the three oppositions covered during HST's first five years. Specifically, the HST data reveal intricate details of cloud morphology and provide a means for quantitative estimation of polar and equatorial cloud opacities [13], as well as atmospheric dust opacities [14]. The 1994–1995 HST images reveal ubiquitous clouds in association with major orographic features, as well as a near-equatorial belt of clouds from -10° to $+30^{\circ}$ latitude. Typical near-equatorial cloud opacities range from 0.25 to 0.35, and higher values occur in association with specific regions like Valles Marineris [13]. Imaging coverage on approximately monthly timescales allows for some study of seasonal variability in condensate behavior. While the HST data are visually stunning and provide important new insights on Mars, all participants agreed that because the HST data are obtained only

infrequently, additional groundbased observations during and between the times of HST image acquisition are essential in order to obtain a complete picture of the time evolution of atmospheric phenomena.

SURFACE OBSERVATIONS

Groundbased observations of the martian surface at reflected solar and thermal emission wavelengths are also producing important new results. One of the main goals of surface observations is to provide constraints on the surface and airborne dust mineralogy. Observations at thermal-IR wavelengths (longward of 5 μm) provide information on primary silicate minerals and on several climatically important secondary minerals, such as carbonates and sulfates [15,16]. Thermal-IR spectroscopic observations from the KAO and IRTF in 1988 and 1990 have revealed evidence for carbonate, sulfate, hydrate, and silicate spectral features [15]. These spectra and newer data from 1993 can also be combined with radiative transfer modeling routines to derive the time evolution of atmospheric dust opacity over the last several apparitions [15]. Thermal-IR imaging spectroscopic observations obtained from Mt. Palomar in 1993 and 1995 reveal spectral variability associated with surface mineralogic differences, although the specific mineralogies involved have not yet been identified [16]. Several participants noted that the Palomar data are the highest-spatial-resolution global thermal-IR spectral data available since the Mariner 9 IRIS measurements, and they will form an important link between previous data and the wealth of new thermal-IR data to be returned by the Mars Global Surveyor TES instrument. Also, as mentioned above, TES will only obtain data for a limited range of local martian time-of-day, centered near 2 a.m. and 2 p.m. for most surface regions. Thus, continued groundbased thermal-IR imaging and spectroscopy will be crucial for studying diurnal variability, which, in combination with the TES data, will help determine the global surface mineralogy and surface/dust thermophysical properties.

Imaging and spectroscopic observations of reflected sunlight at visible and near-IR wavelengths provide information on Fe-bearing silicate minerals, on many secondary minerals and Fe-bearing weathering products, and on condensates and volatile-bearing minerals. Visible-wavelength observations are most sensitive to variations in ferric oxide minerals, which are known to be a constituent of the martian surface as well as important benchmarks of the degree of alteration and weathering history of the surface. A careful choice of visible-imaging wavelengths can allow the detection and discrimination of a number of different mineral phases. Visible CCD multispectral imaging using groundbased telescopes [8] and HST [13,14] provide higher spectral resolution and sampling than the planned Mars Surveyor program visible imaging instruments, and thus these ongoing Earth-based programs will continue to provide unique and useful information that

complements the spacecraft data. In the near-IR, additional information on condensates and volatile-bearing mineral phases can be obtained. Near-IR observations from the IRTF in 1990, 1993, and 1995 reveal evidence for spectral variability related to surface mineralogy or thermophysical property variations, although the specific mineral phases involved have not yet been identified [12]. The specific near-IR wavelengths examined were chosen partly to address the atmospheric science objective discussed above, but also to detect and discriminate specific mineralogic phases like clays, carbonates, and sulfates.

Another active area of Mars surface observational study is the search for and characterization of time-variable phenomena. Examples of such phenomena include the growth and recession of the polar caps, the development of local and global dust storms, and the variations of surface albedo features under the influence of windblown dust. HST observations are providing spectacular new data for assessing these surface changes. Observations of the north polar cap (NPC) recession during 1994–1995 can be directly compared to the NPC recession observed during the same season by Mariner 9 in 1972 [13]. Detailed comparisons between albedo features seen in the recent HST data and in the Viking Orbiter images can be used to assess the stability of different albedo units and to characterize global and local surface dust transport between the late 1970s and the mid 1990s [17]. Recent analyses indicate that many of the large-scale albedo features have changed little over the past several apparitions, or even since the mid 1970s. However, some smaller-scale features, such as Cerberus, appear to have changed substantially [17]. Many workshop participants pointed out the value in comparing imaging data at visible [8,9,11,13,14,17], near-IR [10,12], and thermal-IR [15,16] wavelengths for these time-variable surface regions in order to try to place quantitative limits on the amount of dust cover and/or the mineralogic variability associated with the observed changes.

MODELING AND NUMERICAL STUDIES

Critical to any observational program is a sound understanding of the theoretical basis behind the observations, including knowledge of various hypotheses that the observations will be designed to test. The Mars observational community was fortunate in that a number of theorists and modelers responded to the invitation to participate in the workshop, and these participants were actively involved in the discussions and presentations. For example, there is much that is not known about the chemistry and stability of the martian atmosphere that could be learned by additional, focused, Earth-based studies [18]. Observational constraints on the abundance and distribution of CO, H₂O, O₃, CH₂O, CH₄, H₂, HO₂, and H₂O₂, some of which were discussed above, form the hard constraints on photochemical modeling studies, atmospheric production and loss calculations, and

surface weathering reaction rate models. Much of our current knowledge of Mars atmospheric dynamics and diurnal to interannual surface temperature and pressure variations comes from numerical studies like the NASA Ames General Circulation Model (GCM) [19]. Models like this are designed to fit observational data, and most of the interpretations derived from the GCM are tied to Viking-era observations of Mars. Given that Mars has a dynamic atmosphere and given the evidence for interannual changes in water vapor, dust opacity, albedo, and cloud cover discussed above, it was clear to workshop participants that additional observational constraints for the GCM and similar models based on the current conditions of the planet are needed. An intriguing presentation involving the predicted location of preferred storm zones in the martian polar and midlatitude regions provided a representative example of atmospheric modeling results that could clearly benefit from increased observational constraints [19]. In the case of atmospheric dynamics, the short timescales involved may preclude detailed study by polar-orbiting platforms that observe the planet at a fixed time of day.

CONTRIBUTIONS FROM THE ASSOCIATION OF LUNAR AND PLANETARY OBSERVERS

Unbeknownst to many professional astronomers, there is a small army of skilled and dedicated amateur astronomers worldwide who have equipment and computer resources comparable to those of professionals only a few years ago and who have systematically organized themselves and their observational results. One such organization is the Association of Lunar and Planetary Observers (ALPO), which includes a large and active subsection dedicated to telescopic observations of Mars. Several ALPO members attended the workshop and provided presentations with stunning images and analyses testifying to the skill and usefulness of well-trained "citizen astronomers." One of the goals of the workshop was to foster increased collaborations between the amateur and professional Mars observing communities. It was fabulous to watch these contacts form and develop at the workshop, and it was somewhat amusing and humbling to watch professionals gape at stunning images obtained with a \$500 backyard telescope and CCD system and realize that much of the data in the existing amateur observational databases could be useful for current professional studies.

Much of the focus of the ALPO Mars observational program is on the characterization of surface and atmospheric changes over decade-long timescales. Such studies are possible because of the over 19,000 individual observations of Mars (drawings, photographs, CCD images, and micrometer measurements) collected between 1969 and 1995 by ALPO Mars Section members [20–23]. While any individual, often subjective, observation may not contain a high level of quantitative information, the combination of many tens to hundreds of observations provides a quantitative measure of the

value of qualitative data. These long-duration studies are being used, for example, to compare the NPC retreat in 1994–1995 to the cap retreat seen in previous years [20]. Small differences in the NPC retreat between the 1960s and 1990s are evident, and these differences are thought to be due to the effects of dust in the atmosphere. Especially anomalous behavior was observed in 1984 in association with aphelic dust storms, but this anomalous behavior was not observed during the recent aphelic apparition.

An important and quantitative contribution by amateur observers is the compilation of statistics on the occurrence of various meteorological features, like clouds, hoods, and dust storms [20,23]. Don Parker, an ALPO Mars Section Recorder, noted that he had been puzzled and skeptical for some time over the anomalously high occurrence of clouds during the 1969 apparition, at a season when cloud activity is usually low. However, discussions with professional observers at the workshop (e.g., Barker, Sprague) revealed that the anomalously high cloud activity reported by ALPO observers is correlated with anomalously high water vapor abundances measured on Mars at that time [4]. This is leading to a positive reconsideration of the quality and value of these and other anomalous amateur measurements, in light of corroborating evidence from professional observing programs. Statistics compiled from the more than 2000 Mars observations during 1992–1993 [21,23] and the more than 2500 Mars observations during 1994–1995 [20,22] reveal that there were more frequent and more prominent clouds during 1995 than in 1993, but that the level of cloudiness observed in 1995, though high, was not statistically higher than normal for this season on Mars. Many of the professionals participating in the workshop felt humbled by this result, having believed that 1995 was an exceptionally cloudy opposition. In fact, the ALPO and other long-duration amateur and professional observations indicate that the apparent increase in cloudiness is probably just an artifact arising from a combination of better instrument resolution (CCDs, HST) and the relative inexperience of many professional astronomers who have not been active in the field for more than perhaps one aphelic observing season.

Another important contribution being made by amateur observers and groups such as ALPO is in the study of time-variable surface albedo features. For example, Solis Lacus was observed to be prominent during the late 1980s and early 1990s, but had become small and dark during 1992–1993, only to enlarge and brighten again by 1994–1995 [23]. The prominent dark lane or notch in the NPC known as the Rima Tenuis, seen sometimes as the winter cap begins to sublime, was frequently observed (and photographed) by amateurs during 1994–1995 [20]. These observations of surface albedo changes are often confirmed by professional observers [e.g., 8,9,17]; however, because of the vast advantage in observing time that amateurs enjoy over professionals, high-quality amateur observations of time-variable phenomena can pro-

vide many more details on the processes responsible for the variations observed, and this fact was widely recognized by all participants at the workshop.

Finally, many of the professionals attending the workshop were pleased to hear reports from ALPO observers on the continuing attempts to change the traditional nomenclature from the use of possibly ambiguous and misleading terms like "yellow cloud" or "blue cloud" to more diagnostic descriptions like "localized cloud" or "orographic cloud." Combined with this is an effort by ALPO and several professional observers to convince amateurs to spend more time on dark and flatfield reductions and to begin using standardized (and relatively inexpensive) glass color filter sets, such as the astronomical UBVR set. Not only will this allow for direct intercomparisons of images and color data between different observers and among observations separated by many years, but it will also allow many amateurs with high-quality CCD systems to calibrate their data using easily observed standard stars. Workshop participants realized that once this begins to occur, a new term will have to be coined, because the term "amateur" will no longer apply.

SUMMARY

The ongoing research discussed during the two-day workshop demonstrated that telescopic observers are continuing to gain new insights into important problems in martian surface and atmospheric science. However, major questions still remain regarding atmospheric composition and dynamics, surface composition and mineralogy, and temporal variability on a wide range of timescales. While the ambitious program of planned spacecraft exploration of Mars over the next decade will provide answers to many fundamental questions, specific niches were identified during the workshop in which Earth-based telescopic observations can either augment the spacecraft data in important ways or provide unique measurements and perspectives not possible from orbital or landed platforms. At the end of the two days of technical sessions, there was a general feeling that the workshop had succeeded in its goal of bringing together professional and amateur observers to foster continued collaboration on future Mars telescopic observational projects and on the analysis of previously obtained data. It was pointed out that the workshop was the first major gathering of Mars telescopic observers following an aphelic opposition. Given that so many new and high-quality results were obtained after one of the worst appearances of the planet in 15 years (see cover), participants left the meeting with high hopes that as the apparitions improve substantially over the next decade, so will the quality and quantity of new and exciting discoveries about Mars.

REFERENCES

- All references refer to abstracts of papers presented at the workshop and published in this volume: [1] M. P. Golombek and K. E. Herkenhoff, "Mars Pathfinder Mission, Science Investigations, and Telescopic Observational Support." [2] P. Thomas, "Mars Global Surveyor Camera: Context of Earth-based Observations." [3] K. S. Edgett, T. L. Roush, R. T. Clancy, and P. R. Christensen, "Synergy Between Telescopic Observations of Mars from Earth and the Mars Global Surveyor Thermal Emission Spectrometer." [4] A. Sprague, D. Hunten, and R. Hill, "Spectroscopic Measurements of Atmospheric Water Vapor." [5] M. A. DiSanti and M. J. Mumma, "Atmospheric Water Vapor on Mars: A Search for Enrichment of HDO/H₂O in the North Polar Cap." [6] V. A. Krasnopolsky, M. J. Mumma, and G. L. Bjoraker, "High-Resolution Spectroscopy of Mars at 3.7 and 8 μ m: Hydrogen, Oxygen, and Carbon Isotope Ratios and Implications for Evolution." [7] D. Moreau, A. Marten, J. Rosenqvist, Y. Biraud, and C. Muller, "Millimeter and Infrared Observations of Hydrogenous and Organic Compounds on Mars." [8] L. J. Martin, J. F. Bell III, P. B. James, S. W. Lee, and D. Thompson, "'Mars Watch' Observations from the Lowell Observatory, and Observed Cloudiness in 1994–1995: Possible Implications for Dust Activity." [9] T. Akabane, K. Iwasaki, and L. J. Martin, "Morphologic Features and Opacities of Martian North Polar Hood." [10] D. R. Klassen, J. F. Bell III, and R. R. Howell, "Near-Infrared Imaging Spectroscopy of Clouds and Volatiles." [11] K. E. Herkenhoff and J. Hillier, "Telescopic Determination of Martian Atmospheric Opacity." [12] J. F. Bell III, W. F. Golisch, D. M. Griep, C. D. Kaminski, and T. L. Roush, "Near-Infrared Imaging Spectroscopy of Mars from the IRTF in 1994 and 1995." [13] P. B. James, J. F. Bell III, R. T. Clancy, S. W. Lee, L. J. Martin, and M. J. Wolff, "Hubble Space Telescope Observations of Mars: 1994–1995." [14] D. Crisp, J. F. Bell III, and the WFPC2 Science Team, "WFPC2 Observations of Mars." [15] T. L. Roush, G. C. Sloan, J. F. Bell III, and C. W. Rowland, "Thermal Infrared Spectra of Mars Obtained in 1988, 1990, and 1993." [16] J. Moersch, T. Hayward, P. Nicholson, S. Squyres, and J. Van Cleve, "Thermal Infrared Observations of Mars During the 1995 Opposition." [17] S. W. Lee, M. J. Wolff, P. B. James, L. J. Martin, R. T. Clancy, and J. F. Bell III, "HST Observations of Time-Variable Albedo Features on Mars." [18] S. K. Atreya, "Mars Atmosphere: Chemistry, Stability, and Evolution." [19] J. L. Hollingsworth, R. M. Haberle, A. F. C. Bridger, and J. Schaefer, "Winter Storm Zones on Mars." [20] D. C. Parker and J. D. Beish, "Telescopic Observations of Mars: 1994–1995 Apparition." [21] D. M. Troiani, "The 1992–1993 Apparition of Mars." [22] D. M. Troiani, "The 1994–1995 Apparition of Mars." [23] Presentation by D. Joyce.

Abstracts

MORPHOLOGICAL FEATURES AND OPACITIES OF THE MARTIAN NORTH POLAR HOOD. T. Akabane¹, K. Iwasaki², and L. J. Martin³, ¹Hida Observatory, Kyoto University, Kamitakara, Gifu 506-13, Japan, ²Kyoto-Gakuen University, Kameoka, Kyoto 621, Japan, ³Lowell Observatory, Flagstaff AZ 86001, USA.

We have been observing Mars photographically, and are interested in the polar hoods and polar caps. We are now analyzing the regression of the north polar cap in the 1994–1995 apparition. In the next apparition we plan to observe clouds in the equatorial region. This report describes north polar hood phenomena derived from observations in 1969, 1975, 1986, 1990, and 1992. The season of the northern hemisphere of Mars was early autumn in 1969 and 1986, and was late winter in 1975, 1990, and 1992.

Extent of the Boundary of the North Polar Hood: In the early autumn of Mars the boundary of the north polar hood was not parallel to any latitude line. The boundary extended toward the equator in the morning and receded toward the pole in the afternoon. In 1969 most of the boundaries were around 40°N latitude near 8 MLT (martian local time) and around 60°N about 14 MLT. A similar phenomenon was also observed in late winter in 1990 [1] and 1992. The boundary in 1992 was around 40°N in the morning and about 50°N in the afternoon. The north polar hood recedes during the daytime and may recover either during the night or at dawn. Most boundaries of the polar hood near local noon lay between 40°N and 50°N in 1969 [2]. The mean latitude around local noon was 44°N ± 3° in 1986 (early autumn) and 40°N ± 2°, 35°N ± 5°, and 42°N ± 2°, respectively, in 1975, 1990, and 1992 (late winter). We are also interested in the activity of the north polar hood in late autumn through early winter; however, we had only limited opportunities to observe the polar hood in these seasons due to the tilting of the rotation axis of Mars.

Bright Spots in the North Polar Hood: The north polar hood is always active: Its boundary fluctuates continuously, and its brightness is not uniform. Bright spots often appear in the equatorward region of the polar hood, and appear more frequently in early autumn than in late winter. The boundary of the polar hood sometimes protruded into lower latitudes. Generally the polar hood is not visible in red; however, bright spots are faintly visible in red. The lifetime of bright spots may be less than one day. Most bright spots are not visible near the morning terminator (or limb) on the following day where they should reappear, suggesting that they die out in the late evening or during the night. However, some bright spots survive and reappear the next morning, although with reduced brightness. These surviving spots shift eastward at a rate estimated to be about 700 km/day.

Opacity of the North Polar Hood: The opacity of the polar hood was estimated from the brightness of the polar hood relative to that of the area outside. Using 1969 data, we selected several data points in the hood and a reference point outside the hood near the local noon meridian. It was found that the opacity of the polar hood was high in the early morning and decreased during the day. For example, on July 13, 1969, the opacity at a point (60°N, 195°W) was 1.4 at 8 MLT and decreased to 0.5 at 14 MLT. On July 15, the opacity at the same point was 1.5 at 8 MLT and reduced to 0.4 at 14 MLT. On the average, the opacities around a latitude of 60°N near local

noon were 0.7 ± 0.1 in 1969 and 0.6 ± 0.2 in 1986 [3]. In late winter, the mean opacity was 0.5 ± 0.1 in 1990 [4] and 0.6 ± 0.1 in 1992. There was no significant difference in the opacity of the north polar hood between early autumn and late winter. This suggests that the north polar hood is stable from early autumn through late winter.

Optical Characteristics of the North Polar Hood: The polar hood is seldom seen in red. This fact is consistent with our estimate that its opacity is not high. With a ground albedo of 0.25, the polar hood with opacity of 2 has a contrast of 1.2 in red. This contrast is high enough to be detected easily, and therefore an opaque polar hood should have been easily seen in red. The polar cap in winter is not seen through the hood in blue, suggesting two possibilities: One is that the albedo of the polar cap is too low to be seen through the polar hood, and the other is that the opacity of the polar hood is much higher ($\tau \sim 0.6$) than estimated above. If our value of the opacity of the polar hood is reasonable, the albedo of the polar cap must be less than 0.1 in blue. If, on the contrary, the albedo of the polar cap is higher than 0.3 in blue, the polar hood should be very opaque in blue. Considering that the polar region in winter is not as bright in red as in spring, the albedo of the polar cap may be less than 0.4 in red, and also the opacity of the polar hood should be less than unity in red. If we take the cap albedo of 0.3 over all visible regions, the opacity of the polar hood must be high in blue and low in red, suggesting that the mean size of particles of the polar hood is very small.

References: [1] James P. B. et al. (1994) *Icarus*, 109, 79–101. [2] Martin L. J. and Mckinney W. M. (1974) *Icarus*, 23, 380–387. [3] Akabane T. et al. (1995) *Astron. Astrophys.*, in press. [4] Akabane T. et al. (1993) *Astron. Astrophys.*, 277, 302–308.

MARS ATMOSPHERE: CHEMISTRY, STABILITY, AND EVOLUTION. S. K. Atreya, Department of Atmospheric, Oceanic, and Space Sciences, The University of Michigan, Ann Arbor MI 48109-2143, USA.

The bulk of the atmosphere of Mars is made up of CO₂ (~95%), N₂ (~3%), and Ar (1.6%). O₂ and CO are each at about the 0.1% level. Water vapor and ozone are highly variable with season and location. No definite detection of any hydrocarbons or carbonates is available, although HCHO has been tentatively identified [1]. No suitable oxidant for the surface of Mars has yet been identified, although H₂O₂ and the solar UV are good candidates. Mineralogical data indicate the presence of Cl and S in the surface material and, by implication, in the dust [e.g., 2,3], yet S- and Cl-containing volatiles (such as SO₂, OCS, H₂S, HCl) have not been detected in the atmosphere. Isotopic ratios of O determined from Viking and KAO are different and, if confirmed, may have important implications for the reservoir of O that exchanges with the atmosphere. The D/H ratio needs confirmation and refinement because of its importance in determining the extent of water on early Mars. The measured CO/O₂ ratio is about one-third to one-quarter of that expected from reaction kinetics considerations, and is believed to be regulated by the fluxes of O and H. It is, however, important to have accurate determinations of density distributions of the involved constituents, including H₂. The classical problem of the stability of

martian CO₂ against UV photolysis appears to be largely resolved, with various groups finding the discrepancy between the CO₂ production and loss rates ranging from 10% to 40% [4–6], which is in the noise considering uncertainties in the relevant chemical kinetics data. The oxidation of CO to CO₂ in these models is by OH catalysis [7,8]. Caution should be exercised, however, in interpreting the conclusions of the above “one-dimensional” models, as their results, based on homogeneous gas-phase chemistry, are strictly applicable only to “globally averaged” conditions. Heterogeneous catalysis, as a surface process or as a chemical process, could still play a significant role in the distribution of HO_x and other constituents, as well as in the stability of the atmosphere.

References: [1] Korablev et al. (1993) *Planet. Space Sci.*, 41, 441. [2] Clark et al. (1982) *JGR*, 87, 10059. [3] Blaney and McCord (1995) *JGR*, 100, 14433. [4] Atreya and Gu (1994) *JGR*, 99, 13133. [5] Nair et al. (1994) *Icarus*, 111, 124. [6] Krasnopolsky (1993) *Icarus*, 101, 313. [7] McElroy and Donahue, *Science*, 177, 986. [8] Parkinson and Hunten (1972) *J. Astron. Soc.*, 29, 1380.

NEAR-INFRARED IMAGING SPECTROSCOPY OF MARS FROM THE IRTF IN 1994 AND 1995. J. F. Bell III¹, W. F. Golisch², D. M. Griep², C. D. Kaminski², and T. L. Roush³, ¹Cornell University, Ithaca NY, USA, ²NASA Infrared Telescope Facility, Mauna Kea HI, USA, ³San Francisco State University, San Francisco CA, USA.

We have completed our 1994–1995 program of near-infrared imaging and spectroscopy of Mars from the IRTF on Mauna Kea using the NSFCAM 256 × 256 array camera [1]. The goals of our observing program were to (1) characterize the Mars seasonal volatile cycle by discriminating and spatially mapping H₂O and CO₂ ice clouds and surface hydrated minerals; and (2) perform a high-spatial-resolution, moderate-spectral-resolution search for carbonate, sulfate, or other climatologically diagnostic minerals on the

martian surface and in the airborne dust. Thirteen full or partial nights of IRTF time were granted to this project between September 1994 and April 1995; 10 of these nights produced usable data, including 7 nights where the conditions were photometric and the seeing was subarcsecond (Table 1).

As outlined in Table 1, we obtained data in four different observing modes: (1) imaging through a 0.9% CVF in 32 wavelengths (Nyquist sampled) from 1.560 to 4.100 μm; (2) imaging through a 0.9% CVF in 58 wavelengths from 1.918 to 2.477 μm; (3) imaging through a 1.4% CVF in 48 wavelengths from 3.000 to 4.164 μm; and (4) H-, K-, and L-band slit spectroscopy at R = 500 and through a 0.3-arcsec slit. The 2.5-Gbyte raw dataset is archived on a five-CD set and consists of thousands of Mars, sky, and standard star images, hundreds of Mars, sky, and standard star spectra, and hundreds of flatfield, bias, dark current, and linearity characterization images. All the images were obtained at a spatial scale of 0.06 arcsec/pixel and thus, given the excellent seeing (0.25–0.50 arcsec) that we obtained for several of our observing nights, they have the potential to yield higher-spatial-resolution information than was obtained in our IRTF ProtoCAM imaging during 1990 and 1993 (NSFCAM spatial resolution in 1995 was a maximum of ≈100 km/pixel, as opposed to ≈150 km/pixel using ProtoCAM in 1990 [2]).

We have performed an initial reduction and analysis of a small subset of the data. The data reduction procedures included (1) correction of the raw Mars and standard star imaging data for slight nonlinearity variations inherent in most near-IR InSb array datasets [3]; (2) removal of bias and sky background from the Mars and star images by subtracting an image of an adjacent region of the sky obtained nearly simultaneously; and (3) correction for pixel-to-pixel nonuniformities (flatfield variations) using images of the warm, illuminated inside of the IRTF dome as our flatfield target. The linearized, bias-removed flatfield images are normalized to a mean of 1.0 and divided out of the images from (2). Multiple images (3–5) of Mars and the star were obtained at each wavelength, and these images were examined to see which ones exhibit the best

TABLE 1. Summary of IRTF 1994–1995 Mars Observations.

UT Date YYMMDD	UT Time Range	Size (")	Sub-Earth Lat. (°)	L _s (°)	Mars Longitudes Covered					Data Mode				Comments	
					0	90	180	270	360	1	2	3	4		
940902															Heavy Fog: test data only
941001	1300-1500	6.0	14.4	356	—	—	—	—	—	—	√		√		Some cirrus; seeing 1.2"
941101	1200-1420	7.0	19.0	11	—	—	—	—	—	—	√				Some cirrus; seeing 1.0"
941227	1300-1600	10.7	21.4	37	—	—	—	—	—	—	√	√	√		Photometric; seeing <0.6"
941228	1100-1500	10.8	21.4	37	—	—	—	—	—	—	√		√		Photometric; seeing <0.9"
950114	1200-1540	12.3	20.6	45	—	—	—	—	—	—	√				Photometric; seeing <1.0"
950131															Fog, wind: test data only
950201	0715-1200	13.6	19.3	53	—	—	—	—	—	—	√	√	√		Photometric; seeing <0.8"
950204	0700-1000	13.7	19.0	54	—	—	—	—	—	—	√	√	√		Photometric; seeing <0.6"
950219	0700-1140	13.7	17.7	61	—	—	—	—	—	—	√	√	√		Photometric; seeing <0.7"
950305															Ice storm: no data
950314	0515-1140	12.1	16.6	71	—	—	—	—	—	—	√	√	√		Photometric; seeing <0.9"
950402	0600-1000	10.3	17.2	79	—	—	—	—	—	—	√	√	√		Some cirrus; seeing 1.0"

Data Modes are: 1 = 32-wavelength image set from 1.560 to 4.100 μm (Nyquist sampled)

2 = 58-wavelength image set from 1.918 to 2.477 μm (Nyquist sampled)

3 = 48-wavelength image set from 3.000 to 4.164 μm (Nyquist sampled)

4 = H, K, and L-band slit spectroscopy at R = 500 (0.3 arcsec slit)

resolution (best seeing). The highest-quality images were coadded to increase signal-to-noise (S/N). Sets of images at this level of reduction were registered in orthographic format using simple fractional-pixel shifting. Thus the effects of Mars rotation were not corrected, and analyses were restricted to sets of images obtained closely in time (10–30 min).

Preliminary results show that the north polar regions are bright at 2.25 μm , but very absorbing at 3.00 μm —spectral behavior consistent with the spectrum of water ice. However, at 3.33 and 3.58 μm the situation is more complex, with evidence for high northern latitudinal banding in the images at 3.58 μm and for enigmatic, wavelike features at 3.33 μm . Ratio images of 2.25/3.00 and 2.25/2.432 μm show enhanced polar absorption at 3.00 and 2.432 μm respectively, consistent with an enhanced H_2O abundance associated with the polar hood clouds and/or the subliming polar ice cap. Ratio images of 3.33/3.00 and 3.58/3.00 μm show interesting spatial structure at polar and nonpolar latitudes. It is likely that these features are related to a combination of CO_2 ice and its strong 3.33- μm band, surface thermal properties (important longward of about 3.5 μm on Mars), and other (unidentified) surface mineralogic or atmospheric absorption bands. Finally, the 2.25- μm relative band depth (RBD [2] as defined between 2.21- and 2.278- μm continuum points) map is somewhat correlated with albedo, but shows large variations among different surface regions. The 3.33- μm RBD image (3.20-, 3.58- μm continuum) shows little correlation with albedo and also shows evidence for discrete regions of enhanced polar and limb 3.33- μm absorption that could be caused by CO_2 ice clouds. The 3.45- μm RBD image (3.40-, 3.51- μm continuum) shows interesting polar and midlatitude variations in band strength that correlate with albedo in some places (Syrtris) but not in others (Acidalia).

The complete set of reductions to be performed on the images includes the preliminary steps described above, supplemented by the following procedures: (4) Determination of star flux values using aperture photometry. The raw star data will be scaled to the flux spectrum of BS4030 (35 Leo), assuming a G2 solarlike continuum flux [4]. BS4030 was chosen because it was classified [5] as “very close to solar,” and it was located close to Mars and so allows us to perform both a solar spectrum removal and atmospheric extinction correction. (5) Determination of an atmospheric extinction curve for the star flux spectra derived in (4) using the multiple star observations obtained over a range of airmasses. (6) Scaling of the Mars data from (3) into flux units using the conversion factors derived in (4) and modified for the appropriate Mars airmass using the extinction coefficients derived in (5). By ratioing the Mars flux data with the expected flux from a Lambert surface illuminated by the continuum spectrum of the Sun [6], we can also generate calibrated data in a number of useful planetary photometric units, such as radiance factor [4,7,8]. Calibrating the data into standard flux units will make it possible to compare the data with laboratory sample measurements and previous spacecraft observations, and to extend the interpretations that can be obtained from radiative transfer models that attempt to derive dust opacity and optical properties [9–11]. (7) Map projection onto a standard cylindrical or sinusoidal grid of each of the images in (6) and assembly of calibrated image cubes (spatial \times spatial \times spectral, where the spatial dimension is 256 \times 256 pixels and the spectral dimension is either 32, 48, or 58, depending on the observing mode) from the map-projected data in (7).

References: [1] Shure M. et al. (1994) *Exp. Astron.*, 3, 239–242. [2] Bell J. F. III and Crisp D. (1993) *Icarus*, 104, 2–19. [3] McCaughrean M. (1989) In *Proc. Third Infrared Detector Technology Workshop*, pp. 201–219, NASA TM-102209. [4] Bell J. F. III et al. (1994) *Icarus*, 111, 106–123. [5] Hardorp J. (1978) *Astron. Astrophys.*, 63, 383–390. [6] Smith E. V. P. and Gottlieb D. M. (1974) *Space Sci. Rev.*, 16, 771–802. [7] Hapke B. (1981) *JGR*, 86, 3039–3054. [8] Roush T. L. et al. (1992) *Icarus*, 99, 42–50. [9] Herkenhoff K. E. (1993) *Bull. AAS*, 25, 1061–1062. [10] Ockert-Bell M. E. et al. (1994) *Bull. AAS*, 26, 1130. [11] Pollack J. B. et al. (1995) *JGR*, 100, 5235–5250.

WFPC2 OBSERVATIONS OF MARS. D. Crisp¹, J. F. Bell III², and the WFPC Science Team¹, ¹Jet Propulsion Laboratory, Pasadena CA, USA, ²Cornell University, Ithaca NY, USA.

We used the Hubble Space Telescope (HST) Wide Field/Planetary Camera-2 (WFPC2) to take images of Mars on February 24–27, 1995, just after opposition. Mars was imaged at ultraviolet (160, 255, 336 nm) and near-infrared (1042 nm) wavelengths to place improved constraints on the airborne dust and ice optical depths and the ozone column abundances. These images are also being used to produce high-spatial-resolution maps of the surface CO_2 and H_2O frost deposits and other surface albedo features. Planetary Camera images were taken at four sub-Earth longitudes ($\sim 22^\circ$, 94° , 231° , and 311°) to provide near-global coverage with a minimum of foreshortening.

The near-ultraviolet images at 255 and 336 nm reveal a dark martian surface with a bright north polar cap and bright water ice clouds. The ice clouds are concentrated near the morning and evening limbs and at latitudes south of 50° , forming a south polar hood. A few discrete bright clouds were also seen near the Tharsis volcanos and over Elysium Mons. The morning limb was in shadow at the surface, but the atmosphere was still illuminated at altitudes above ~ 25 km. The clouds near the morning limb are confined below this altitude. In contrast, there is a high-altitude detached haze layer on the evening limb. The south polar hood is much darker at 255 nm than at 336 nm. This darkening has been attributed to enhanced ozone absorption at these latitudes.

The 1042-nm images reveal the well-known bright and dark albedo markings. The surface and atmospheric ices are much less apparent at this wavelength. For example, the north polar cap is only 75% as bright as the brightest regions of Elysium. The relatively bright, red, airborne dust is more easily detected, however. The largest dust optical depths are seen over the relatively dark, heavily cratered terrain just south of the equator.

ATMOSPHERIC WATER VAPOR ON MARS: A SEARCH FOR ENRICHMENT OF HDO/ H_2O IN THE NORTH POLAR CAP. M. A. DiSanti¹ and M. J. Mumma², ¹Universities Space Research Association/Goddard Space Flight Center, Code 693, Greenbelt MD 20771, USA, ²NASA Goddard Space Flight Center, Code 690, Greenbelt MD 20771, USA.

We present a method for obtaining latitudinally resolved spectra of atmospheric H_2O and deuterated water (HDO) on Mars, which should permit us to address the question of whether HDO is en-

riched in the polar ice caps. To demonstrate our method, we show examples of near-IR H₂O and HDO long-slit spectra from the 1993 apparition.

Existing models developed for the odd-hydrogen chemical cycle on Mars have neglected the role of transport within the atmosphere. We have been investigating this problem with the use of spatially resolved global maps of CO, H₂O, HDO, and CO₂ absorption lines to assess transport and photochemistry in the martian atmosphere. A major goal of our program is to assess the seasonal and global behavior of water vapor. In particular, we wish to test some of the major findings of the Viking Orbiter Mars Atmospheric Water Vapor (MAWD) experiment [1,2]. These include (1) there are no local sources or sinks of water vapor, except at the poles; (2) there is a notable asymmetry in the water behavior with respect to latitude, with the northern hemisphere containing up to twice as much vapor as the southern hemisphere; and (3) the average annual column abundance of water tracks the local topography, the lowest altitudes having the most vapor and the highest having the least. Although the observed major north-south gradient in water vapor implies a net annual flow of water toward the south, it is not known whether this flow is balanced by other terms (e.g., transport in the form of water ice clouds or when adsorbed onto airborne dust grains), nor is it known whether the vapor patterns measured during the Viking mission are representative of other martian years.

In addition to its importance to the photochemistry of Mars, the isotopic information stored in HDO and H₂O is an important indicator of atmospheric escape. The deuterium-to-hydrogen (D/H) ratio is a key measure of atmospheric evolution for the terrestrial planets. The initial value of D/H depends upon the primordial volatile inventory. Over geologic time D/H is modified by mass-selective processes such as Jeans escape and hydrodynamic outflow, and perhaps by cometary impacts. The D/H ratio on Mars is of particular interest because an accurate estimate of the atmospheric value may help to constrain the size of the exchangeable reservoir of water in the regolith and polar caps.

Deuterated water was first detected on Mars by Owen et al. [3] using the Canada-France-Hawaii telescope on Mauna Kea. The product of airmass (η) and abundance (a) was estimated to be $\eta a(\text{HDO}) = (3.6 \pm 0.8) \times 10^{-2}$ pr μm . In order to derive the D/H ratio, a measurement of H₂O is required, but this is very difficult from the ground because of terrestrial extinction. Using doppler-shifted H₂O lines near 1.1 μm , Owen et al. measured $\eta a(\text{H}_2\text{O}) = 20 \pm 8$ pr μm . The resulting value for D/H was $(9 \pm 4) \times 10^{-4}$, indicating an enhancement of 6 ± 3 over the value in terrestrial oceans. The large uncertainty resulted from the need to make measurements of the Moon and Mars on different days because of long integration times. We are attempting to avoid this difficulty by using Mars itself to calibrate terrestrial extinction (see below).

Bjoraker and Mumma, in collaboration with H. P. Larson, simultaneously measured HDO and H₂O on Mars in August 1988, when $L_s = 246^\circ$ (late spring in the southern hemisphere), using NASA's Kuiper Airborne Observatory (KAO). The global average value for D/H was found to be enhanced by a factor of 5.15 ± 0.15 relative to terrestrial (SMOW). Virtually all the atmospheric water on Mars at that time was sublimated from the southern polar cap.

It is not known whether water is transported from one cap to the other as the seasons change, nor whether the D/H ratio in the southern polar cap is also representative of the northern polar cap. These questions can be addressed by measuring the ratio of HDO/

H₂O as a function of latitude and martian season. Because of their different zero-point energies, HDO has a significantly lower saturation vapor pressure than does H₂O. Therefore HDO condenses first as the temperature falls and vaporizes more slowly as the frost is warmed. This could cause net distillation of HDO toward the polar caps, and might lead to preferential sequestering of HDO in the caps and in the regolith at high latitudes. Furthermore, the obliquity of Mars and its current orbital configuration are such that the southern polar cap receives on average less solar insolation than does the northern. With the vapor pressure isotope effect, deuterium may migrate to the south polar cap over geologic time. Our measurements can constrain this potentially very important effect.

We observed Mars on March 9–12, 1993 (UT), using CSHELL ($\lambda/\Delta\lambda \sim 2 \times 10^4$) at the IRTF. At this time $L_s \sim 50^\circ$, or northern spring; thus the north polar cap would have just begun to sublimate. Based on MAWD measurements, virtually no water vapor is expected at southern latitudes for this L_s value. We oriented the 30-arcsec-long slit north-south, allowing full latitudinal coverage over the disk of Mars (which subtended ~ 9 arcsec), and established two beam positions (A and B) by nodding the telescope 15 arcsec along slit between integrations. Frame differences (A–B) accomplished first-order sky subtraction.

A principal advantage in using modern array detectors is that they provide *simultaneous* spatial coverage for extended objects. We targeted the H₂O 111–000 band at 8820 cm^{-1} , and the HDO ν_1 band at 2720 cm^{-1} . At the time of our observations, Mars had a geocentric velocity of ~ 16 km s^{-1} , which doppler shifted the martian water lines into the wings of the corresponding terrestrial absorptions. We have been experimenting with the use of southern latitude spectra as calibrators of terrestrial extinction to determine whether HDO is preferentially sequestered in the northern polar ice cap reservoir. We expect this method to be applicable to data obtained during seasons in which the water vapor is strongly concentrated above one of the polar caps. For other seasons (e.g., when L_s is near 0° or 180°) an external calibrator, such as the lunar spectrum obtained at an air mass comparable to Mars, is required.

References: [1] Farmer C. B. et al. (1977) *JGR*, 82, 4225–4248. [2] Jakosky B. M. and Farmer C. B. (1982) *JGR*, 87, 2999–3019. [3] Owen T. et al. (1988) *Science*, 240, 1767–1770.

SYNERGY BETWEEN TELESCOPIC OBSERVATIONS OF MARS FROM EARTH AND THE MARS GLOBAL SURVEYOR THERMAL EMISSION SPECTROMETER. K. S. Edgett¹, T. L. Roush², R. T. Clancy³, and P. R. Christensen¹, ¹Department of Geology, Arizona State University, Box 871404, Tempe AZ, 85287-1404, USA, ²Department of Geosciences, San Francisco State University and NASA Ames Research Center, Mail Stop 245-3, Moffett Field CA 94035-1000, USA, ³Space Science Institute, Suite 294, 1234 Innovation Drive, Boulder CO 80303-0588, USA.

The Mars Global Surveyor (MGS) thermal emission spectrometer (TES) will obtain middle-infrared spectra of the martian surface and atmosphere [1]. This report discusses the potential for synergy between telescopic observations made from Earth/Earth orbit and those that will be obtained by TES. Ironically, TES has its roots in the Earth-based radiometric observations of Mars in the 1920s by Pettit and Nicholson [2] and Coblentz and Lampland [3–

4). Coblentz was also the "father" of middle-infrared spectroscopy of inorganic materials [5].

The Mars Global Surveyor is scheduled for a November 1996 launch, with arrival at Mars in September 1997. The mapping phase begins January 1998, when the spacecraft is in a nearly circular, polar orbit (367 km altitude, 93° inclination, period of 117 minutes with a 7-day repeat cycle). The primary mission is to observe the planet for an entire martian year; an extended mission could begin in January 2000.

TES consists of three subsections: a Michelson interferometer, a solar reflectance sensor (0.3–2.7 μm), and a thermal bolometer (5.5–100 μm). The spectrometer covers the middle-infrared region from 6 to 50 μm ($\sim 1600\text{--}200\text{ cm}^{-1}$) with 5 and 10 cm^{-1} spectral resolution options. The spectrometer has six uncooled DTGS pyroelectric detectors in a 3×2 array, each with $\sim 3\text{-km}$ ground resolution at nadir for the 367-km-altitude orbit. TES is being fabricated at the Hughes Santa Barbara Research Center in Goleta, California, for an April 1996 delivery date.

The specific objectives of TES are to determine (1) the mineral composition of the surface; (2) the composition, particle size, and spatial/temporal distribution of suspended dust; (3) the location, temperature, height, and water abundance of H_2O clouds; (4) the composition, seasonal behavior, total energy balance, and physical properties of the polar caps; and (5) the particle size and distribution of rocks and fines on the surface [1]. TES will build up a global image of Mars over multiple orbits, taking ~ 200 days to obtain full coverage at the equator.

There are two kinds of telescopic observations that will be valuable when used in conjunction with TES: (1) existing telescopic data and (2) new observations to be obtained while MGS is in orbit. New observations that might be obtained 1997–2005 that would be most relevant to enhancement of TES objectives include radar and perhaps continued monitoring of weather conditions. The next four paragraphs suggest some points for synergy in terms of martian climate, surface properties, mineralogy, and landing site selection. These points are for discussion purposes and do not reflect a specific plan for coordination between TES and new telescope observation strategies.

Monitoring Weather: Telescopic monitoring of weather provides continuity with observations of Mars dating back more than 100 years. One need only recall Mariner 9 in 1971, which reached Mars just as Earth-based observations showed a major dust storm. The Mariner 9 IRIS ("grandfather" of TES) obtained many observations of suspended dust, providing our first information about the composition and optical properties of dust storms [6–7]. However, since the 1970s it has become "clear" that the martian atmosphere is not always as dusty and warm as it was then. Microwave CO spectra from groundbased radio telescopes have yielded temperature profiles (0–70 km altitude) of the Mars atmosphere [8–9] since 1980. Apart from global dust storms in 1992 and 1994 [10], these measurements show a Mars atmosphere that is 15–20 K colder than in the 1970s. Microwave profiles of Mars atmospheric water also suggest a colder, less dusty Mars atmosphere, in which water saturates at low altitudes [9]. Hubble Space Telescope imaging and spectroscopic observations also show evidence of this behavior through images of globally extended clouds [9,11] and increased atmospheric ozone levels during northern spring/summer. Earth-based thermal-IR spectral cameras will be useful during the TES mission because they have the capability of providing relatively

rapid measurement of the entire Earth-facing hemisphere, providing short-timescale (hourly) monitoring of the development and evolution of local and global atmospheric phenomena (e.g., dust storms), plus longer-timescale (months to years) monitoring of interannual variability of atmospheric phenomena (e.g., atmospheric dust loading). These Earth-based atmospheric measurements relate directly to the capability of TES to measure and monitor atmospheric temperature, water, clouds, and ozone. TES should provide a much more detailed view of the "new" Mars climate in the context of the longer-term groundbased studies of the Mars atmosphere.

Surface Physical Properties: TES will provide thermophysical information. Earth-based radar provides important information about physical properties that complement thermal infrared observations [e.g., 12]. The relatively recent development of radar imaging capabilities for Mars have led to the discovery of "stealth" features, which may be voluminous volcanic ash deposits [13–15]. TES can provide information that will lead to better characterization of "stealth." Radar images might also serve as a means complementary to TES for monitoring polar cap development, particularly beneath a polar hood.

Surface Mineral Properties: The main objective of TES is to obtain surface mineral composition. Existing telescopic data provide clues as to the presence of pyroxenes, hematite, etc. [e.g., 16], and have led to predictions about the nature or composition of Mars surfaces [e.g., 17]. TES will obtain data at a single time of day/night, but new observations from Earth can be made during the MGS mission that sample various times of day, providing the ability to obtain information from the same surface region at different temperatures and atmospheric conditions; such information can be useful for separating relative spectral contributions from surface and atmosphere constituents [e.g., 18]. Finally, airborne and Earth-orbiting thermal-IR observations can obtain data at wavelengths where the TES signal-to-noise ratio is low, such as $\leq 6.25\ \mu\text{m}$, where there are spectral features diagnostic of hydrates and some carbonates [e.g., 18–20].

Mars Surveyor Landing Site Selection: Radar observations are potential "show stoppers" in the process of landing site selection, and have been very important for assessing the proposed Mars Pathfinder landing site [e.g., 21]. TES observations of physical and compositional properties, in combination with radar observations, will likely play major roles in the site selection process for the 1998–2005 Mars Surveyor landers.

References: [1] Christensen P. R. et al. (1992) *JGR*, 97, 7719–7734. [2] Pettit E. and Nicholson S. B. (1924) *Pop. Astron.*, 32, 601–608. [3] Coblentz W. W. (1922) *Proc. Natl. Acad. Sci. U.S.*, 8, 330–333. [4] Coblentz W. W. and Lampland C. O. (1924) *Pop. Astron.*, 32, 570–572. [5] Coblentz W. W. (1906) *Carnegie Inst. Wash. Publ.*, 65. [6] Hanel R. A. et al. (1972) *Science*, 175, 305–309. [7] Toon O. B. et al. (1977) *Icarus*, 30, 663–696. [8] Clancy R. T. et al. (1990) *JGR*, 95, 14543–14554. [9] Clancy R. T. et al. (1995) *Icarus*, submitted. [10] Clancy R. T. et al. (1994) *Bull. AAS*, 26, 1130. [11] James P. B. et al. (1994) *Icarus*, 109, 79–101. [12] Jakosky B. M. and Christensen P. R. (1986) *JGR*, 91, 3547–3559. [13] Muhleman D. O. et al. (1991) *Science*, 253, 1508–1513. [14] Butler B. J. (1994) Ph.D. dissertation, California Institute of Technology. [15] Zimbelman J. R. and Edgett K. S. (1994) *Eos Trans. AGU*, 75, 217. [16] Singer R. B. et al. (1979) *JGR*, 84, 8415–8426. [17] Merényi E. et al. (1995) *Icarus*, submitted. [18] Pollack J. B. et al. (1990) *JGR*, 95, 14595–14627. [19] Soderblom L. A.

(1992) in *Mars* (H. H. Kieffer et al., eds.), pp. 557–593, Univ. of Arizona, Tucson. [20] Calvin W. M. et al. (1994) *JGR*, 99, 14659–14675. [21] Harmon J. K. and Campbell B. A. (1995) in *LPI Tech Rpt. 95-01, Part 1*, 17–18.

MARS PATHFINDER MISSION, SCIENCE INVESTIGATIONS, AND TELESCOPIC OBSERVATIONAL SUPPORT.

M. P. Golombek and K. E. Herkenhoff, Jet Propulsion Laboratory, California Institute of Technology, Pasadena CA 91109, USA.

Mars Pathfinder is one of the first Discovery-class missions, which are quick, low-cost projects with focused science objectives. In addition to demonstrating an inexpensive system for cruise, entry, descent, and landing on Mars (July 1997), it will deploy and operate a micro-rover and three science instruments: a stereoscopic imager with visible through near-infrared filters on a pop-up mast, an alpha proton X-ray spectrometer (APXS), and an atmospheric structure instrument/meteorology package. This payload provides the opportunity for carrying out a variety of scientific investigations, including surface morphology and geology at meter scale, elemental composition and mineralogy of surface materials, and a variety of atmospheric science investigations.

The Pathfinder flight system is an aircraft consisting of a simple backpack-style cruise stage, deceleration subsystems, and a tetrahedron-shaped lander packaged within the aeroshell and backcover. The spacecraft enters the martian atmosphere directly from an Earth-Mars transfer trajectory and is slowed by the aeroshell and parachute. The lander is lowered on a tether below the backcover and parachute. Prior to landing, three small solid rockets fire, the tether is cut, and the lander impact is cushioned by inflated airbags. After coming to rest, the airbags are deflated and retracted and the triangular petals open, righting the lander, exposing solar panels, and allowing the rover to drive off. The lander is capable of surviving for at least 30 sols, with a possible lifetime of up to a year.

The rover on Mars Pathfinder is a small (10-kg), six-wheel-drive rocker-bogie-design vehicle. It is a solar-powered vehicle that operates almost entirely within view of the lander cameras (a few tens of meters). The payload consists of monochrome stereo forward cameras for hazard detection and terrain imaging and a single rear color camera. Also on the rear of the vehicle is the APXS, which is mounted on a deployment device that will place the APXS sensor head against both rocks and soil. The APXS and the visible to near-infrared (0.4–1 μm) filters on the lander imaging system will determine the elemental composition and constrain the mineralogy (particularly pyroxene and iron oxides) of rocks and other surface materials, which can be used to address questions concerning the composition of the crust, its differentiation, and the development of weathering products.

The atmospheric structure instrument will determine pressure, temperature, and density profiles of the atmosphere (with respect to altitude) during entry and descent at a new location, time, and season (landing will occur in southeast Chryse Planitia, 600 km from Viking Lander 1, just before sunrise in late northern summer). Measurements of pressure and temperature will be made in a triangular space between the petals at the base of the lander during descent. Redundant three-axis accelerometers will allow extraction of atmospheric density profiles and hence pressure and temperature profiles during entry. Diurnal variations in the atmospheric bound-

ary layer will be characterized by regular surface meteorology measurements (pressure, temperature, atmospheric opacity, and wind). Three thermocouples will be mounted on a 1-m-high mast located on a petal away from the thermally contaminating lander electronics to determine the ambient temperature profile with altitude. A wind sensor on the top of this mast, along with three wind socks below it, will allow determination of wind speed and direction vs. altitude in the boundary layer and calculation of the aerodynamic roughness of the surface. Regular sky and solar spectral observations by the lander imager will also monitor dust particle size and shape, refractive index, vertical aerosol distribution, and water vapor abundance.

Following an open workshop [1], the landing site selected for Pathfinder is Ares Vallis (19.5°N, 32.8°W, -2 km elevation), where a catastrophic flood channel debouches into Chryse Planitia. This site is a “grab bag” site with the potential for sampling a wide variety of different martian crustal materials, such as Noachian plateau material (ancient crust) as well as Hesperian ridged plains and a variety of reworked channel materials. Even though the exact provenance of the samples would not be known, data from subsequent orbital remote sensing missions could then be used to infer the provenance for the “ground truth” samples studied by Pathfinder.

The surface and atmospheric models used by the Pathfinder project to optimize entry, descent, and landing (EDL) and surface operations are based primarily on Viking Lander data. However, it has been recognized that recent observations of Mars indicate that its atmosphere is significantly colder and clearer than during the Viking missions [3]. Because EDL sequencing depends on the density of atmospheric gases and aerosols, information regarding the temperature and opacity of the martian atmosphere just before Pathfinder’s arrival is strongly desired. Such data will also be useful in planning surface operations early in the landed mission, as lander and rover power depend on the insolation at the surface and radiative transfer in the atmosphere. Power is needed to keep electronics warm during the cold martian night, so unusually low surface temperatures will decrease the power available for telecommunications. Hence, the amount of data that can be returned to Earth, and therefore operational scenarios, will depend on the amount of dust in the martian atmosphere. Groundbased and Earth-orbital observations of Mars atmospheric temperature and opacity during the spring of 1997 would greatly aid in Pathfinder mission planning. In addition, observations of Mars during the Pathfinder mission with the landing site near the sub-Earth point would allow Pathfinder observations to be placed in a global context. Conversely, Pathfinder data will be useful in calibrating telescopic observations of martian atmospheric opacity and temperatures.

References: [1] Golombek M., ed. (1994) *LPI Tech. Rpt. 94-04*, 49 pp. [2] Golombek M. et al. (1995) *LPS XXVI*, 481. [3] Clancy R. T. et al. (1995) *Icarus*, submitted.

TELESCOPIC DETERMINATION OF MARTIAN ATMOSPHERIC OPACITY. K. E. Herkenhoff and J. Hillier, Mail Stop 183-501, Jet Propulsion Laboratory, California Institute of Technology, Pasadena CA 91109, USA.

The amount of dust in the martian atmosphere is variable in both space and time [1,2]. The presence of aerosols in Mars’ atmosphere complicates quantitative analysis of martian surface properties [3–

7]. Dust storms have been observed telescopically for almost 200 years, and are known to have major effects upon the structure and circulation of the martian atmosphere [8,9]. Great dust storms tend to occur during the southern spring and summer [2], and may be an important mechanism by which dust is transported into the polar regions [10]. It is widely believed that the martian polar layered deposits record climate variations over at least the last 10–100 m.y. [11–18], but the details of the processes involved and their relative roles in layer formation and evolution remain obscure [19]. The layered deposits are widely believed to be the result of variations in the proportions of dust and water ice deposited over many climate cycles [13–15]. However, the amount of dust currently transported into the polar regions is unknown, as are the effects of global climate changes on dust transport. In order to infer the climate history of Mars from geologic evidence, including the polar layered deposits, the current cycling of dust through the martian atmosphere must be understood. Long-term, continuous monitoring of martian atmospheric dust opacity is therefore desired in order to address these questions. In addition, future missions to Mars (including possible human exploration) will require better knowledge of the likelihood and severity of martian dust storms.

Zurek and Martin [2] found that “planet-encircling dust storms do not occur every Mars year, and . . . that there may have been periods of several successive years without such storms.” The clarity of Mars images taken during recent oppositions suggests that the martian atmosphere has been less dusty recently than in previous years [20]. Ingersoll and Lyons [21] proposed that martian great dust storms are chaotic phenomena, influenced by the amount of “background” dust in the atmosphere. However, their analysis was hindered by gaps in the historical record of martian dust opacity. Martian dust storms can be detected from the ground only when Mars is relatively close to Earth, so a complete seasonal or interannual history of dust storms is impossible to obtain from groundbased data alone. The optical depth of aerosols in the martian atmosphere between dust storms has been determined primarily from Mars spacecraft data [22,23], but can also be inferred from groundbased [5] and Earth-orbital observations [24]. Hubble Space Telescope images of Mars show that the dust opacity was less than 0.06 in December 1990 [25]. We have initiated a collaborative effort with Mars astronomers using HST images to test and refine our Mars photometric model. Our previously developed model for Mars surface and atmospheric scattering was based on equations (1) through (6) in Hillier et al. [26,27]. This formulation was chosen for its speed of computation and because it accounts for the spherical geometry of atmospheric scattering at high emission angles, i.e., near the planetary limb. However, the atmosphere is assumed to be optically thin in this model, so optical depths greater than 0.2 cannot be modeled using this formulation. We are therefore modifying a three-dimensional radiative transfer code at JPL to more realistically model groundbased, HST, and Viking Orbiter images of Mars. Recently derived dust optical properties [28,29] will initially be used and tested against the observational data. This technique holds promise for determining martian atmospheric opacity over a large fraction of the martian year, thus allowing better definition of the global dust cycle and its interannual variability.

References: [1] Martin L. J. and Zurek R. W. (1993) *JGR*, 98, 3221. [2] Zurek R. W. and Martin L. J. (1993) *JGR*, 98, 3247. [3] Arvidson R. E. et al. (1989) *JGR*, 94, 1573. [4] Herkenhoff K. E. and Murray B. C. (1990) *JGR*, 95, 1343. [5] Lumme K. (1976)

Icarus, 29, 69. [6] Thorpe T. E. (1978) *Icarus*, 36, 204. [7] Thorpe T. E. (1982) *Icarus*, 49, 398. [8] Gierasch P. J. and Goody R. M. (1972) *J. Atmos. Sci.*, 29, 400. [9] Haberle R. M. et al. (1982) *Icarus*, 50, 322. [10] Barnes J. R. (1990) *JGR*, 95, 1381. [11] Murray B. C. et al. (1972) *Icarus*, 17, 328. [12] Cutts J. A. et al. (1976) *Science*, 194, 1329. [13] Cutts J. A. et al. (1979) *JGR*, 84, 2975. [14] Squyres S. W. (1979) *Icarus*, 40, 244. [15] Toon O. B. et al. (1980) *Icarus*, 44, 552. [16] Carr M. H. (1982) *Icarus*, 50, 129. [17] Howard A. D. et al. (1982) *Icarus*, 50, 161. [18] Plaut J. J. et al. (1988) *Icarus*, 75, 357. [19] Thomas P. et al. (1992) in *Mars* (H. H. Kieffer et al., eds.), pp. 767–795, Univ. of Arizona, Tucson. [20] Martin L. J. et al. (1991) *Bull. AAS*, 23, 1217. [21] Ingersoll A. P. and Lyons J. R. (1991) *Bull. AAS*, 23, 1217. [22] Zurek R. W. (1982) *Icarus*, 50, 288. [23] Esposito L. W. et al. (1990) *Bull. AAS*, 22, 1076. [24] Lee S. W. et al. (1993) *Bull. AAS*, 25, 1031. [25] Clancy R. T. (1992) personal communication. [26] Hillier J. et al. (1991) *JGR*, 96, 19203. [27] Herkenhoff K. E. and Martin L. J. (1993) *Bull. AAS*, 25, 1061. [28] Pollack J. B. et al. (1995) *JGR*, 100, 5235. [29] Clancy R. T. et al. (1995) *JGR*, 100, 5251.

WINTER STORM ZONES ON MARS. J. L. Hollingsworth^{1,2}, R. M. Haberle², A. F. C. Bridger³, and J. Schaeffer⁴, ¹San Jose State University, San Jose CA 95192, USA, ²NASA Ames Research Center, Moffett Field CA 94035, USA, ³Meteorology Department, San Jose State University, San Jose CA 95192, USA, ⁴Sterling Software, Inc., Palo Alto CA 94393, USA.

In meteorology, a storm track typically is defined as the path taken at the surface by weather cyclones—high- and low-pressure centers and associated frontal zones—as they travel from west to east in winter middle latitudes. The phrase may also denote longitudinally or latitudinally confined regions within the atmosphere where such transient disturbances preferentially develop or decay. When referring to such geographically confined regions, the term storm zone may be more appropriate. These zones can be identified in high-frequency eddy statistics, e.g., time-filtered variance and covariance fields of momentum and temperature [1]. Growth and decay of the transient disturbances are accepted to hinge on baroclinic and barotropic processes, specific dynamical instabilities within the atmosphere wherein large-scale eddies act as the dominant mechanism for the transport of heat, momentum, and moisture in winter midlatitudes [2–4]. Tracks taken by surface low-pressure centers can be associated with upper-level eddy temperature and momentum variance and covariance fields, and particularly in the northern hemisphere, storm zones occupy a finite longitude band. The western part corresponds to regions of genesis of the disturbances and the eastern part corresponds to where the systems occlude and decay [3].

Mars’ atmospheric circulation reveals similar yet also very different features compared to those found on Earth [5]. In both atmospheres solar differential heating drives Hadley circulation cells with rising motion in low latitudes, poleward motion aloft, sinking motion in middle latitudes, and a return flow near the surface toward the subtropics [6]. In addition to Hadley circulations, both planets exhibit thermally indirect (eddy-driven) circulation cells in winter middle and high latitudes. Viking observations have demonstrated that Mars’ winter atmosphere, like Earth’s, exhibits traveling weather systems associated with the process of baroclinic instability [7]. Such transient eddies have very regular lifecycles compared to those

on Earth, and their poleward transports of heat and momentum strongly influence the global atmospheric energy budget [8]. Earth and Mars both exhibit large-scale orography and, in a broadly defined context, “continents.” Great orographic complexes will cause significant latitudinal excursions of the seasonally averaged atmospheric flow [9]. In Mars’ northern hemisphere, the large-scale orographic features are the high-relief regions in middle latitudes (the protrusions of Tharsis in the western hemisphere, Arabia Terra and Elysium in the eastern hemisphere) and Vastitas Borealis in high latitudes (a longitude-encircling “trough” on the order of 1 km below the 6.1 mbar standard topographic datum). In Mars’ southern hemisphere, Tharsis and the low relief in the Argyre and Hellas basins constitute the primary features. Although Mars lacks oceans, longitudinal variations in the planet’s surface albedo and thermal inertia fields support “thermal” continents that can also affect the time-mean circulation [5].

Atmospheric general circulation models are effective tools that can be applied in studies of a planet’s circulation and the nature of its climate. Using the NASA Ames Mars general circulation model (MGCM) [6,8], we investigate whether Mars’ midlatitude winter transient eddies can occur in preferred geographic regions. We focus, in particular, on two northern winter simulations with moderate dust loading: (1) one with full spatial variations in topography, surface albedo, and thermal inertia and (2) one with no topography but with varying thermal fields as in (1). Our objectives are to identify whether storm zones may be expected to occur and, if they do, to determine which physical mechanisms, mechanical, thermal, or both, could account for any geographic regionalization.

As shown in Fig. 1, our simulations indicate that Mars’ orography plays a dominant role in localizing transient eddy activity. This figure depicts the low-pass, time-filtered north-south (meridional) wind variance from the simulation with full surface variations. Compelling evidence that the midlatitude eddies grow and decay in preferred regions can be seen: the strongest variance occurs near 45°W longitude, on the eastern edge of Tharsis; weaker maxima are found near 150°W and 120°E. The highlands in the eastern hemi-

sphere are distinctly more quiescent. These storm zones imply locales for volatile and dust transport and correspond to regions likely to be cloudier and dustier than adjacent areas. They may thus be key regions in the planet’s dust and water cycles. In contrast, the simulation without topography (not shown), reveals little localization of transient (co)variance fields.

Observational support of the storm zone patterns may exist in data obtained from the Mariner 9 and Viking spacecrafts. High correlations exist between bright wind streak orientation and MGCM surface stress in middle and low latitudes [10]. There is also a strong correlation between high rock abundance and strong near-surface winds. Both are consistent with fine surface material swept free [10]. “Wave” and “streak” condensate clouds are evidenced in Mariner 9 and Viking Orbiter images and they appear to occur near the same longitudes as the MGCM storm zones [11,12]. Full-disk images of Mars in UV wavelengths (255–410 nm) obtained with HST, although for northern spring season, also show that organized large-scale cloud streaks and clusters occur in Arcadia Planitia and north of the Tharsis plateau [13]. Complete coverage of cloud type as a function of geographic location and season provided by HST and future orbiting spacecraft will better establish the strength of this correlation.

References: [1] James I. N. (1994) *Introduction to Circulating Atmospheres*, Cambridge Univ. [2] Wallace J. M. et al. (1988) *J. Atmos. Sci.*, 45, 439–462. [3] Hoskins B. J. et al. (1983) *J. Atmos. Sci.*, 40, 1595–1612. [4] Peixoto J. P. and Oort A. H. (1992) *Physics of Climate*, Am. Inst. Physics. [5] Leovy C. B. (1985) *Adv. Geophys.*, A28, 327–346. [6] Haberle R. M. et al. (1993) *JGR*, 98, 3093–3124. [7] Barnes J. R. (1980) *J. Atmos. Sci.*, 37, 2002–2015. [8] Barnes J. R. et al. (1993) *JGR*, 98, 3125–3148. [9] Hollingsworth J. L. and Barnes J. R. (1995) *J. Atmos. Sci.*, in press. [10] Greeley R. et al. (1992) in *Mars* (H. H. Kieffer et al., eds.), 730–766, Univ. of Arizona, Tucson. [11] French R. G. et al. (1981) *Icarus*, 50, 468–493. [12] Kahn R. (1983) *JGR*, 88, 10189–10209. [13] Bell J. (1995) personal communication.

HUBBLE SPACE TELESCOPE OBSERVATIONS OF MARS: 1994–1995. P. B. James¹, J. F. Bell III², R. T. Clancy³, S. W. Lee⁴, L. J. Martin⁵, and M. J. Wolff¹, ¹University of Toledo, Toledo OH 43606, USA, ²Cornell University, Ithaca NY 14853, USA, ³Space Science Institute, Boulder CO 80309, USA, ⁴Laboratory for Atmospheric and Space Physics, University of Colorado, Boulder CO 80309, USA, ⁵Lowell Observatory, Flagstaff AZ 86001, USA.

Mars was monitored by the Hubble Space Telescope approximately once per month between August 1994 and August 1995. This was a continuation of a program of synoptic martian observations that commenced in December 1990 [1] and has included all periods in which the solar elongation of the planet has exceeded the 50° HST limit. The 1994–1995 observations are summarized in Table 1.

All these sequences prior to July 1995 include exposures using five filters with bandpasses centered at 255, 336, 410, 502, and 673 nm. Additional filters were used in July. The sub-Earth latitude varied between a minimum of about 5° in August 1994 to a maximum of more than 26° in July 1995; thus the best views were of regions in the northern hemisphere, and a good record of the late-winter to mid-summer regression of the north polar cap was therefore obtained.

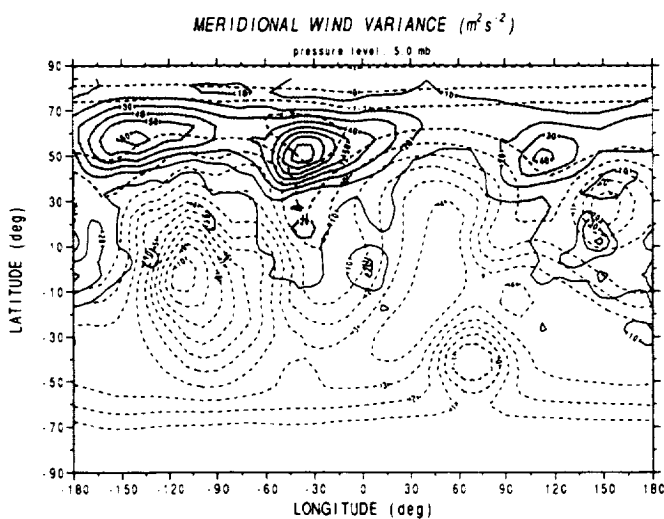


Fig. 1. North-south wind variance (m^2/s^2) from a northern winter simulation. Contour intervals are 1 km and $10 \text{ m}^2/\text{s}^2$ for topography (dashed) and variance respectively.

TABLE 1. Summary of 1994–1995 observations.

Date	L_s	CML	$D(^{\circ})$	θ_c
08/23/94	335.7	289.1	5.18	5.08
09/19/94	349.7	274.8	5.67	11.83
10/20/94	5.2	284.3	6.53	17.55
11/18/94	19.1	277.2	7.80	21.03
01/02/95	39.9	280.2	11.21	21.75
02/24/95	63.4	275.9	13.48	17.68
02/25/95	63.5	34.5	13.46	17.66
02/25/95	63.7	151.8	13.44	17.64
04/08/95	82.3	282.5	9.80	18.15
05/28/95	104.1	272.0	6.77	23.56
07/06/95	122.1	276.6	5.55	23.33
07/06/95	122.2	34.1	5.54	26.34
07/11/95	124.8	159.2	5.42	26.43

The most salient feature of the martian atmosphere during the period of these observations was the appearance of a planet-encircling belt of clouds after $L_s = 60$, as seen in Fig. 1. Concentrations of clouds clearly exist near the martian volcanos, in the classic “W cloud” locations, but these are superimposed on a general band of clouds extending from about -10° latitude to 30° latitude with maximum opacity occurring at about 20° . The 410-nm opacity of the clouds at 20° latitude is generally between 0.25 and 0.35 except in the vicinity of 65° W longitude, where the opacity is between 0.4 and 0.5 over a broad range of latitudes; this corresponds to the Valles Marineris canyon system.

The season in which these ubiquitous clouds were seen is near northern summer solstice, where general circulation models [2] predict a strong Hadley circulation with ascending branch in the northern subtropics, where these clouds are concentrated. This is also the period when Mars is closest to the aphelion of its orbit, and the reduced insolation could, especially in the absence of widespread planetary dust, result in water saturation and condensation at fairly low levels in the atmosphere. These clouds could be a significant impediment to the transport of water from the northern to the southern hemisphere by the Hadley circulation during this season, when the largest amounts of vapor are observed on the planet in the northern hemisphere [3], and could therefore be significant factors in the net water transfer between hemispheres [4].

An interesting exception to the pattern of bluish clouds in the northern subtropics was seen in the April 1995 HST images, which show a fairly extensive region of dust haze in the northern plains adjacent to the retreating north polar cap. An extensive regional

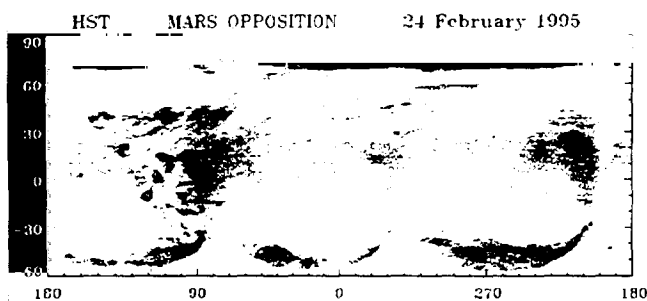


Fig. 1.

storm was seen by Viking during this same season the year following the major 1977 planet-encircling dust storms. The equatorial cloud belt is much less conspicuous in the April images, suggesting perhaps that the vertical temperature profile in the subtropics has been modified by dust absorption. As can be seen in the subsequent May image, the planet had returned to its previous clouded state, which persisted in the incompletely processed July images. In fact, the cloud over the southern Syrtis Major region in the May image appears to be one of the more optically thick clouds we have seen on the planet in terms of the contrast changes that it produces.

The 1994–1995 images provide an excellent record of a north polar cap recession that can be compared with prior observations. The opposition sequence provided the opportunity to view the entire polar cap at an L_s identical to Mariner 9 views in 1972. The sizes and shapes of the caps in the two years seem to be very similar. In particular, the cap displays the “peculiar polygonal” outline alluded to by the Mariner 9 teams, and the frost coverage in the interior of the cap is clearly patchy as in 1972, though the smaller resolution of the HST images relative to the Mariner 9 frames does not permit a detailed comparison of bright and dark areas. The crater Korolev is conspicuous as a bright outlier in both datasets.

References: [1] James P. B. et al. (1994) *Icarus*, 109, 79–101. [2] Haberle R. M. et al. (1993) *JGR*, 98, 3093–3123. [3] Jakosky B. M. (1985) *Space Sci. Rev.*, 41, 131–200. [4] Clancy R. T. et al. (1995) *Icarus*, submitted. [5] Soderblom L. A. et al. (1973) *JGR*, 78, 4197–4210.

NEAR-INFRARED IMAGING SPECTROSCOPY OF CLOUDS AND VOLATILES. D. R. Klassen¹, J. F. Bell III², and R. R. Howell¹, ¹University of Wyoming, Laramie WY 82070, USA, ²Cornell University, Ithaca NY 14850, USA.

Recent Hubble imaging of Mars in the visible and near-UV has shown a thermal environment differing from past experience that can be better addressed by groundbased infrared imaging spectroscopy. The Hubble images show a planet covered with clouds in a season when the higher atmospheric temperatures should preclude such formations. The north polar cap is also still evident. These images indicate a much colder martian spring than during the Viking age.

Although Hubble can easily image the clouds and polar cap, due to its wavelength limitations it cannot distinguish between H_2O and CO_2 ices. These volatiles do have several significant absorption bands in the near-infrared and it is in this region that they can be distinguished [1]. Spectral imaging in the infrared will allow us to map and follow these absorption features, and thus to follow the clouds and the polar cap and to distinguish their compositions.

We have spectral imaging sets taken throughout the past opposition, acquired using the NSFCAM at the NASA Infrared Telescope Facility. NSFCAM is equipped with CVFs that allow spectral imaging from 1.3 to $4.3 \mu m$ at a spectral resolution of around 1.5–2.0%. The seasonal coverage is from $L_s = 356$ to $L_s = 79$ (almost the entire spring season).

In this study we will concentrate on images in and around major H_2O and CO_2 absorption bands. The region near $3.00 \mu m$ is used for the detection of H_2O as there is a strong water ice feature but only a weak CO_2 feature. The region around $3.33 \mu m$ is used to detect

CO₂ ice clouds due to its strong narrow absorption feature. In this region, water ice has a relatively low, flat reflectance [1].

Presented here are preliminary results based on relative band depth (RBD) maps created from the images in and around the major absorption features [2]. These maps will show the spatial and temporal variations in the H₂O and CO₂ ice clouds as well as the north polar cap.

References: [1] Bell J. F. et al. (1995) *JGR*, submitted.
[2] Bell J. F. and Crisp D. (1993) *Icarus*, 104, 2–19.

HIGH-RESOLUTION SPECTROSCOPY OF MARS AT 3.7 AND 8 μm: HYDROGEN, OXYGEN, AND CARBON ISOTOPE RATIOS AND IMPLICATIONS FOR EVOLUTION. V. A. Krasnopolsky, M. J. Mumma, and G. L. Bjoraker, NASA Goddard Space Flight Center, Greenbelt MD 20771, USA.

A combination of the KPNO 4-m telescope and Fourier transform spectrometer with the GSFC postdisperser was used to observe low-latitude regions of Mars in the spectral ranges of 2650–2800 cm⁻¹ and 1229–1237 cm⁻¹ with resolving power $\nu/\delta\nu = 2.7 \times 10^5$ and 1.2×10^5 respectively. The main spectral features are isotopic lines of CO₂ and HDO lines. A radiation transfer code has been developed that divides the atmosphere into 30 layers and the Voigt profile of each line in each layer into 60 intervals. This code couples the reflected solar and thermal radiations. The observed HDO lines result in an abundance that, when compared with that of H₂O measured by the Vikings at the same season and latitudes, yields an enrichment in the D/H ratio of a factor of 6 ± 2 relative to the Earth. The given uncertainty is mainly caused by possible year-to-year variations of Mars' atmospheric water abundance. Methane abundance on Mars is rather uncertain: 70 ± 50 ppb, not significantly different from the Mariner 9 upper limit of 20 ppb and smaller than the 2σ upper limit of our measurements. Formaldehyde should be the main intermediate product of CH₄ decomposition, with H₂CO/CH₄ $\approx 3 \times 10^{-6}$. The upper limit of H₂CO measured by us is equal to 3 ppb, which is much smaller than recently claimed abundances. A search for H₂O₂ lines at 1229–1237 cm⁻¹ results in an upper limit of 30 ppb and imposes some constraints to models of the martian

TABLE 1. Main results of the measurements.

Result	Comment
D/H = 6 ± 2	In water vapor, scaled to SMOW
¹⁸ O/ ¹⁷ O = 0.916 ± 0.04	In CO ₂ , scaled to terrestrial CO ₂
¹³ C/ ¹² C = 1.02 ± 0.14	In CO ₂ , scaled to terrestrial CO ₂
CH ₄ = 70 ± 50 ppb	Smaller than the 2σ upper limit and consistent with the Mariner 9: CH ₄ < 20 ppb
H ₂ O ₂ < 30 ppb	Recent photochemistry gives 10–40 ppb
H ₂ CO < 3 ppb	2σ limit
HCl < 2 ppb	Previous limit was 100 ppb

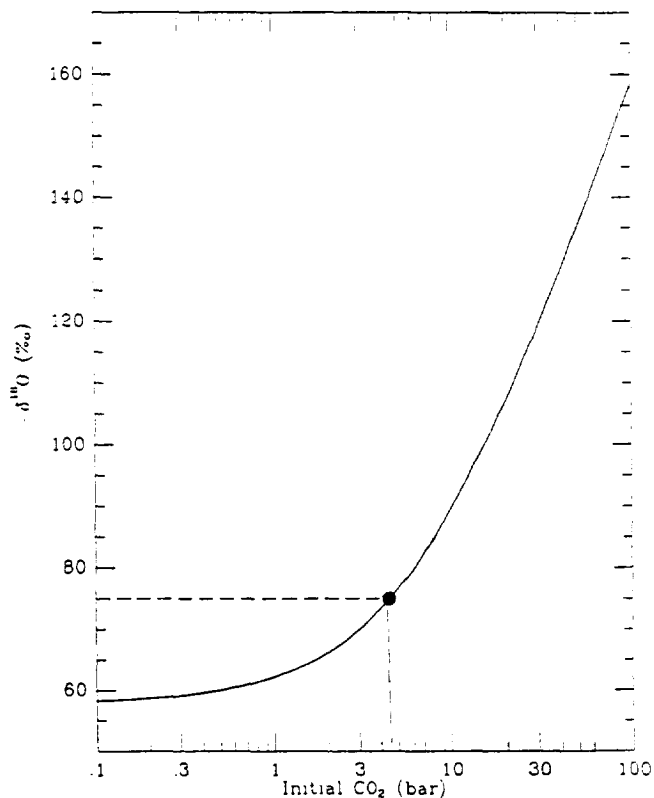


Fig. 1. Depletion in heavy O in the present atmosphere as function of the initial CO₂ abundance in the case of impact erosion of the atmosphere. The measured weighted-mean depletion of 75‰ corresponds to 5 bar of CO₂.

photochemistry. The measured upper limit of HCl < 2 ppb precludes any significant Cl chemistry in the atmosphere.

The measurements revealed ≈ 200 lines of the CO₂ isotopes 628, 627, and 638 with 38 lines absent in databases. Eighty lines of the three isotopes with close equivalent widths were chosen to determine the O and C isotope ratios in CO₂. The measured ratios are ¹⁸O/¹⁷O = 0.916 ± 0.04 and ¹³C/¹²C = 1.02 ± 0.14 scaled to CO₂ in the Earth's atmosphere. Scaling to SMOW and assuming the same initial isotope ratio on Mars and Earth, we find that ¹⁸O/¹⁶O = 0.88 ± 0.07 in CO₂ on Mars. Comparison with the same value in H₂O on Mars shows that photochemical exchange of O between CO₂ and H₂O is stronger than thermodynamic isotope equilibrium. Combined with other measurements, these ratios result in weighted-mean atmospheric ratios of ¹⁸O/¹⁶O = 0.925 ± 0.028 and of ¹³C/¹²C = 0.972 ± 0.045 relative to the terrestrial standards. Two processes affect the C isotope ratio in the atmosphere: formation of carbonates and C escape. To explain the O isotope ratio, we take into account all processes depleting this ratio: water-silicate, vapor-ice, and water-CO₂-carbonate equilibria. Assuming the water endowment of 0.5 km, the water escape of 30 m, and the CO₂ escape of 43 mbar, we consider two scenarios of atmospheric evolution: with and without intense erosion by meteorite and planetesimal cratering in the first 0.8 b.y. In both cases initial abundance of CO₂ deduced from the C and O isotope ratios on Mars exceeds that in the present atmosphere by 3 orders of magnitude and was equal to 5 bar for ¹⁸O/¹⁶O = 0.925 in the case of impact erosion. The CO₂ abundance was in the range of 0.3–1 bar at the end of impact erosion at 0.8 b.y. based on the measured ¹³C/¹²C.

HST OBSERVATIONS OF TIME-VARIABLE ALBEDO FEATURES ON MARS. S. W. Lee¹, M. J. Wolff², P. B. James², L. J. Martin³, R. T. Clancy⁴, and J. F. Bell III⁵, ¹Laboratory for Atmospheric and Space Physics, University of Colorado, Boulder CO 80309, USA, ²University of Toledo, Toledo OH 43606, USA, ³Lowell Observatory, Flagstaff AZ 86001, USA, ⁴Space Science Institute, Boulder CO 80309, USA, ⁵Cornell University, Ithaca NY 14853, USA.

The Mariner 9 and Viking missions provided abundant evidence that eolian processes are active over much of the surface of Mars [1–4]. The primary manifestation of this activity observable from the vicinity of Earth is in the form of variable albedo features. In 1990, a long-term program of HST observations commenced to monitor the surface and atmosphere of Mars [5,6]. To date, slightly more than two martian years of observations have been obtained.

The Syrtis Major region exhibited a great deal of variability in albedo during the Viking missions [cf. 4], hence it was chosen as the primary target for repeated observations by HST. Since December 1990, the appearance of this region has varied only slightly; certainly none of the major albedo variations noted during Viking have been observed [5]. The variability during Viking was probably related to the major dust storms that occurred several times during that mission. The current “stability” of the region indicates that dust activity of a magnitude comparable to that during Viking has not occurred since the HST observations commenced. Observations indicate that the Solis Planum region, also noted for albedo variability, also has not undergone major changes in albedo features.

One major albedo feature that has changed dramatically between the Viking period and present is Cerberus. This feature was observed to be relatively constant in appearance between the Mariner 9 and Viking missions [7]. However, in the February 1995 HST

observations, Cerberus had virtually disappeared (see Fig. 1). This indicates that the normally dark surface has been covered with bright dust sometime during the period between Viking (ending in 1982) and the present. Initial examination of our HST observations indicates that Cerberus has not been prominent in any images obtained since 1990. We will be collaborating with other groundbased observers to determine when this feature began to fade, and whether this variability can be traced to any observed dust storm activity in the region.

References: [1] Veverka J. et al. (1977) *JGR*, 82, 4167–4187. [2] Thomas P. et al. (1981) *Icarus*, 45, 124–153. [3] Greeley R. et al. (1992) in *Mars* (H. Kieffer et al., eds.), pp. 730–766, Univ. of Arizona, Tucson. [4] Kahn R. et al. (1992) in *Mars* (H. Kieffer et al., eds.), pp. 1017–1053, Univ. of Arizona, Tucson. [5] James P. B. et al. (1994) *Icarus*, 109, 79–101. [6] James P. B. et al., this volume. [7] Chaikin A. L. et al. (1981) *Icarus*, 45, 167–178. [8] Pleskot L. K. and Miner E. D. (1981) *Icarus*, 45, 179–201.

“MARS WATCH” OBSERVATIONS FROM THE LOWELL OBSERVATORY, AND OBSERVED CLOUDINESS IN 1994–1995: POSSIBLE IMPLICATIONS FOR DUST ACTIVITY. L. J. Martin¹, J. F. Bell III², P. B. James³, S. W. Lee⁴, and D. Thompson¹, ¹Lowell Observatory, Flagstaff AZ, USA, ²Cornell University, Ithaca NY, USA, ³University of Toledo, Toledo OH, USA, ⁴University of Colorado, Boulder CO, USA.

The 1994–1995 Mars apparition was observed at the 31" telescope at Lowell Observatory between mid October and early June by various combinations of the listed authors. During this period we obtained telescope time for 19 observing runs of 3 to 6 nights each, totaling 43 scheduled nights. We acquired Mars images on 18 of

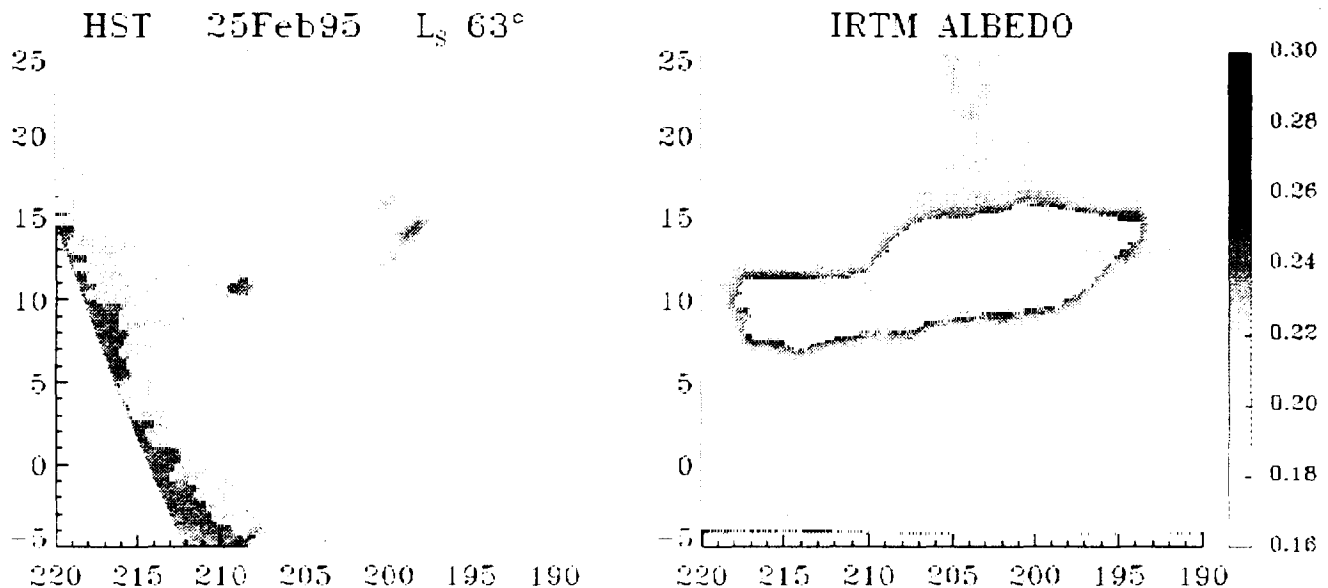


Fig. 1. Comparison of the appearance of the Cerberus albedo feature in HST and Viking observations. Maps are in simple cylindrical projection. The IRTM phase-corrected albedo map is from the Mars Consortium data collection [8]; the brightness scale to the right refers only to this IRTM map. The HST map was produced from a 673 nm image obtained in Feb. 1995. A Minnaert correction has been applied ($k = 0.65$), and data at emission angles greater than 75° have been eliminated. It is evident that much of the cerberus albedo feature is not visible at the time of the HST observations.

those nights, and although this was a respectable 42%, not all those nights yielded usable images. We experienced our share of unfavorable winter weather and the poor "seeing" that often develops between storms.

All observations were made using the Lowell Observatory occultation CCD camera and software written by M. Buie of Lowell. The automated filter wheel for this camera system provided space for nine filters and an open position that was used to aid in finding Mars each night. We selected a mix of nine wide- and narrowband filters to suit the maximum possible uses for the various interests of the observers. These ranged from 4400 Å to 10,400 Å. Exposure times for the different filters were from a maximum shutter speed of about 20 ms to 15 s. The image was enlarged about four times by using a Planetary Patrol Barlow lens system in front of the camera.

Observing sequences were automated by a macros program written by S. Lee. This allowed us to run through one of two filter combinations, automatically setting exposure times and triggering the shutter for multiple exposures (9 each for the full set of filters and 20 each for a preselected set of 4 more commonly used filters). The smaller set was used when conditions were less favorable. Since seeing conditions fluctuate rapidly, some images are always better than others.

New technology may have shortcomings that must be analyzed and compensated for. Because this camera is electronically cooled and operated, it includes two electronic boxes that must also be mounted to the telescope's tailpiece. These boxes generate a small amount of heat that is exhausted into the dome, thus adding to turbulence known as "dome seeing," probably degrading the image definition. With help of Lowell's engineer, R. Nye, we improvised a solution by placing a hood (plastic tarp) around the tailpiece to isolate the temperature differential and exhausted that air out of the dome with an extension hose on a common vacuum cleaner. In spite of all the sophistication of new instrumentation, we must ascertain that we do not pay the price of obtaining high quantities of second-rate data, and sometimes a low-tech solution may be appropriate.

We estimate that these data include several thousand Mars images. We are now in the process of reducing and analyzing these data. Lee has modified an IDL program for use in expediting this reduction and analysis. This enables us to select the more useful images from multiple, same-time exposures of 9–20 images. These images, together with those from other sources, are used to evaluate the changes in the surface and atmosphere of Mars that took place during this apparition. This dataset will also be merged with images obtained by Parker and others. These data are crucial for filling the time gaps between the more detailed but infrequent Hubble Mars observations. Since we get images of the same face of Mars with the Hubble camera at intervals exceeding a month and of other sides only a couple of times each apparition, these groundbased observations can often tell us what happened during the periods between. They are proving to be very useful in determining the short-term histories of various cloud, polar cap, and albedo phenomena.

Cloudiness in 1994–1995: Various researchers have noted that Mars was very cloudy during this past apparition, and some have made some suggestions relating to the possible implications that this may have regarding dust storms. It is noted that some of the Viking approach imaging along with other early Viking Orbiter imaging showed rather widespread cloudiness on Mars prior to and during the early phases of the first 1977 planet-encircling dust storm [1]. Prior to this storm, the limb clouds and hazes were seen to

rapidly increase in elevation [2]. In comparing the fourth day of the 1971 and 1973 planet-encircling storms, together with the 1977 storm on Viking Orbiter 178B images, we see that all three storms included bright condensate clouds in and around the bright dust clouds [3,4]. The relationships between "red" clouds, "blue" clouds, and "ultraviolet" clouds continued through the expansion phases of the 1971 and 1973 storms [5,6], during which the dust storms encircled Mars. As these storms then matured, the condensate clouds that had been seen in blue and ultraviolet apparently dissipated. These condensate clouds seem to have played a role in the development of the dust storms. It seems possible that turbulence from those clouds could have been a factor in raising dust. Since the initial clouds of these storms were bright through all the visible range of filters, those clouds may have been composed of both dust and condensates. The high amount of cloudiness during this past apparition may have been uncommon, but is not unprecedented, and probably does not indicate a reduced probability for dust activity.

References: [1] Briggs G. et al. (1977) *JGR*, 82, 4121–4149. [2] Martin L. J. et al. (1991) in *LPI Tech. Rpt. 92-02*. [3] Martin L. J. and Baum W. A. (1978) *Bull. AAS*, 10, 551. [4] Martin L. J. (1981) *Bull. AAS*, 13, 708. [5] Martin L. J. (1974) *Icarus*, 22, 175–188. [6] Martin L. J. (1976) *Icarus*, 29, 363–380.

MILLIMETER AND INFRARED OBSERVATIONS OF HYDROGENOUS AND ORGANIC COMPOUNDS ON MARS.

D. Moreau¹, A. Marten², J. Rosenqvist², Y. Biraud², and C. Muller¹,
¹Belgian Institute for Space Aeronomy, Belgium, ²Observatoire de Paris Meudon, France.

Introduction: In 1989 solar occultation observations of the martian atmosphere by the Auguste experiment onboard the Phobos spacecraft provided infrared spectra showing new absorption features not detected previously that were interpreted as HCHO signatures [1]. Since this tentative detection was uncertain, Moreau et al. [2] proposed a list of potential C-H bond compounds by using an updated version of a two-dimensional model of the martian atmosphere [3]. However, a strong constraint on the formation of such gases is the abundance of CH₄. The recent CH₄ detection by Krasnopolsky [4], with a mixing ratio estimated between 20 and 120 ppb, allows us to reinterpret these observations.

Another key point of martian aeronomy concerns the abundances of hydrogenous compounds. Specifically, to explain the chemical stability of the atmosphere of Mars, a mechanism was first proposed by Parkinson and Hunten [5] invoking the reaction of CO with OH radicals produced by the photolysis of mainly H₂O₂ and HO₂. This catalytic mechanism predicts an H₂O₂ mixing ratio ranging between 0.01 ppm and 0.1 ppm at the surface and an HO₂ mixing ratio of at least 1 order of magnitude lower. It appears that H₂O₂ may be the key constituent for the photochemical regulation of H₂, O₂, and CO. Nevertheless, no detection of H₂O₂ or HO₂ of any sort has been performed so far.

Millimeter Observations: Martian heterodyne observations were carried out with the IRAM 30-m telescope (Spain, Granada) at four epochs: May 1992, December 1992, December 1994, and January 1995. Several compounds, such as CH₂O, H₂O₂, HO₂, CH₃OH, which exhibit spectral signatures in the millimeter range, have been searched for [6]. Originally, we tried to confirm Phobos

detection of HCHO from specific observations conducted in 1992, but no line was detected. During the subsequent observing runs performed with new observational techniques we were not able to detect any line. The first information extracted from these observations is an upper limit of HCHO concentration at least 3 orders of magnitude less than that retrieved from Phobos data. However, determination of this upper limit is not substantially in disagreement with the Phobos observation. Study of all abundance estimates in comparison with the theoretical results of our photochemical model seems to indicate that the high concentration of organic molecules observed during the Phobos mission could apparently be a local process related to heterogeneous catalytic processes at the surface and/or on airborne dust [7]. However, the nondetection in the microwave range implies that more refined studies on the source of the organic precursor of HCHO in the current martian atmosphere have to be done. The very stringent constraint derived from the millimeter observations of H_2O_2 has a significant impact on martian photochemistry. Because H_2O_2 number density is partly linked to H_2O atmospheric concentration, a simple hypothesis is to consider strong variations of the global water vapor amount in the martian atmosphere at the epoch of the observations (December 1994–January 1995). Conversely, this result should suggest a possible basic problem in our understanding of martian photochemistry. The H_2O_2 upper limit we derived suggests either a very low global H_2O amount in the atmosphere or a peculiar concentration in the lower atmosphere that limits the H_2O photolysis. Nondetection of H_2O_2 and HO_2 could be perceived as evidence of an increase of the condensation processes of H_2O_2 and/or a decrease of the desorbed water from the regolith. In both cases, these results must be envisaged as closely related to a modification of the global thermal structure as well as to a modification of the dust loading of the atmosphere. Moreover, a low concentration of water could have a significant feedback on the oxidizing capacity and thus on the catalytic cycle of stabilization of the current martian atmosphere.

Infrared Observations: The Infrared Space Observatory (ISO), which is a scientific project of the European Space Agency (ESA), is scheduled to be launched by ARIANE 4 in September 1995. It will carry out astronomical observations in the 2.5–240- μm range with four instruments. Martian observations are represented by one of the guaranteed time proposals, while our observing proposal is accepted as a target of opportunity in the case of martian global storms. Basically, it consists of the observation of Mars with many payload instruments during dust storms. If operational limits appear, a preference will be given to the short wavelength spectrometer (SWS) covering the 2.5–45- μm band. Martian dust storms can occur during the ISO lifetime but cannot be predicted with certainty far in advance. During storm periods, the photochemistry of the martian atmosphere will be deeply modified due to radiative feedbacks and catalytic reactions on airborne dust. The thermal structure of the atmosphere is not well known during these storms, while most models predict a global warming locally. Cooling could also occur, leading to a modification of the balance of water vapor. The martian chemistry, as discovered by the Mariner, Mars, Viking, and Phobos missions, is much more complex than expected earlier as exemplified by our tentative identification of organic compounds. The ISO payload presents the best way to monitor it from the Earth's orbit. This proposal asks for a complete martian observation with the instrumental payload using the same survey mode and same means

as the martian guaranteed time proposal but on a target-of-opportunity mode. The feasibility is actually better than for the original guaranteed time proposal by which it is inspired since the planet is more radiatively active during dust storms and its atmospheric temperature in some regions is significantly higher than commonly. The study of martian dust storms is about a century old but theories have only appeared in the last 20 years. Before a dust storm perturbed the start of the Mariner 9 mission, the storms had never been studied from space. The present Hubble Space Telescope payload now allows a good UV and visible survey of Mars, but even with new NICMOS foreseen in the future, the lack of infrared coverage limits the chemical study of specific phenomena during storms. On the other hand, the near- and far-infrared capabilities of ISO will permit us to investigate the surface in a great number of mineralogically significant bands of various materials. Groundbased telescopes, even if their instruments have much improved the detection possibilities, are still limited to the atmospheric windows, and accordingly compete with the infrared capabilities of ISO.

References: [1] Korabiev O. et al. (1993) *Planet. Space Sci.*, 152, 33. [2] Moreau D. et al. (1992) *Bull. AAS*, 24, 1015. [3] Moreau D. et al. (1991) *JGR*, 96, 7933. [4] Krasnopolsky V. A. (1995) *Annal. Geophys.*, 13, 753. [5] Parkinson T. D. and Hunten D. M. (1972) *J. Astron. Soc.*, 29, 1380. [6] Marten A. et al. (1995) in preparation. [7] Moreau D. (1995) Thesis.

THERMAL INFRARED OBSERVATIONS OF MARS DURING THE 1995 OPPOSITION. J. Moersch, T. Hayward, P. Nicholson, S. Squyres, and J. Van Cleve, Center for Radiophysics and Space Research, Cornell University, Ithaca NY 14853, USA.

Using the SpectroCam-10 instrument on the Hale 200" telescope at Palomar Observatory, we obtained an extensive set of images and spectra of Mars in the thermal infrared during the 1995 opposition. Images were taken using a set of seven wideband filters centered at 7.9, 8.8, 9.8, 10.3, 11.7, 12.5, and 17.9 μm over a wide range of central meridians on the nights of February 16, 27, and 28 (UT). Spatially resolved slit spectra with a wavelength resolution of $\lambda/\Delta\lambda = 200$ between 7.5 and 13.5 μm were also obtained covering the entire disk at several central meridians.

Several final data products are being constructed from this dataset, including 11 image cubes, 10 spectral cubes, a spectral map of the planet covering $\sim 140^\circ$ of longitude at constant insolation geometry (constructed from spectral slits aligned on the central meridian), and a planet rotation movie at 11.7 μm .

A much smaller set of similar observations carried out with SpectraCam in a test run during the 1993 opposition led to the identification of an absorption feature at 9 μm in the Acidalia region [1]. At the time the feature was first identified, it was impossible to determine whether it was caused by a local enhancement of atmospheric dust over Acidalia, or by non-unit emissivity of surface materials in that region. A major goal for the 1995 campaign was to reobserve this part of the planet to determine if the 9- μm feature persists. Early analyses of 1995 imaging data indicate that the feature does persist, and is therefore most likely to be of surficial origin. Analysis of 1995 spectral mode data for the Acidalia region is currently underway.

References: [1] Moersch J. E. et al. (1994) *LPS XXV*, 569.

TELESCOPIC OBSERVATIONS OF MARS: 1994–1995 APPARITION. D. C. Parker and J. D. Beish, Mars Recorder, Association of Lunar and Planetary Observers, 12911 Lerida Street, Coral Gables FL 33156, USA.

Our research during the 1994–1995 Mars apparition has concentrated on martian meteorology and north polar cap (NPC) behavior. Measurements of the NPC areocentric latitude were obtained between 22° and 112° L_s from 220 bifilar micrometer and 168 red-light CCD images. While the cap latitudes obtained from CCD measurements averaged 1.3° lower than those measured with the micrometer, the differences were not significant (P = 0.36). In addition, the 36 measurements submitted from red-light video images were not significantly different from the micrometer or CCD sets (P = 0.84). The resulting regression curve for the 1994–1995 apparition is fairly smooth, lacking significant periods of retardation (Fig. 1).

The 1995 NPC regression was statistically compared to those obtained during previous apparitions. Through 60° L_s the 1995 curve was virtually identical to that obtained by Viking in 1978 [1]. Analysis of the 1980 [2], 1982 [3], and 1984 [4] regressions with both paired and unpaired nonparametric tests reveal that the 1995 north cap was consistently and significantly smaller for a given L_s. When the cap latitudes were merged into 5° L_s increments, the 1995 NPC averaged 4.8° latitude smaller than the combined values from the 1980s (Fig. 2), using the Wilcoxon signed rank test (P < 0.01). The 1984 regression displayed unusual retardations between 60° and 110° L_s, a period coinciding with the appearances of five localized aphelic dust storms [5] (see Fig. 3). Even with the 1984 data omitted, the 1995 cap still averaged 2.9° latitude smaller (P < 0.01). When all the raw data from the 1980s are combined and compared to those of 1995 between 22° and 112° L_s, there is no statistical difference. However, this appears mainly due to the coincidence of values for the summer cap. The 1995 spring (24°–90° L_s) cap is 2.4° latitude smaller than the combined 1980 and 1982 values (P < 0.05 > 0.01). It appears that the 1995 cap started out smaller but regressed at a slower rate (0.36° areocentric latitude/°L_s) than the 1980 and 1982 caps (0.45°/°L_s) during the period between 45° and 90° L_s.

The NPC regressions of the 1960s [6] reveal consistently larger caps than the 1980s or 1995 at a given L_s (Fig. 2), despite considerable overlap in personnel, equipment, and technique. These data have been corrected for the revised axial tilt determined by Mariner 9 data. During the 1969 apparition, the NPC displayed unusual regrowth near aphelion and between 100° and 120° L_s [7]. Even

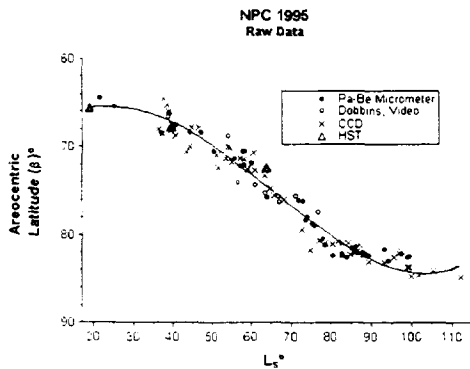


Fig. 1.

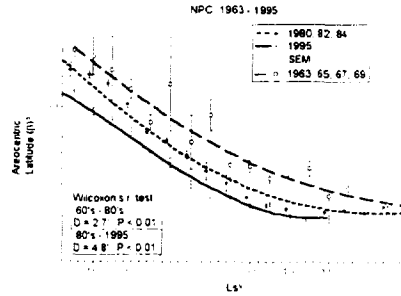


Fig. 2.

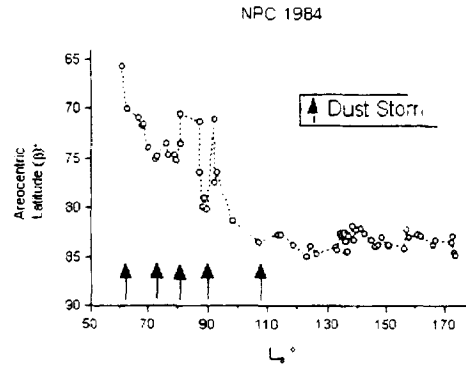


Fig. 3.

without the 1969 data, the 1960s north cap latitude averaged 2.0° (Wilcoxon) and 2.4° (Mann-Whitney) larger than those of the 1980s (P < 0.01).

Over 200 tricolor CCD images of Mars were obtained and analyzed for meteorological phenomena and included in our ongoing study [8]. Although our statistical analysis is not complete for the 1994–1995 apparition, there was a widespread cloudiness on all sides of Mars. Equatorial band clouds, previously thought to be rare, were especially prevalent. Whether this was real or merely the result of better imaging and visual observations remains to be seen. Some interesting relationships between meteorology and NPC behavior appear to be emerging from our meteorological study, which now includes approximately 19,000 observations made over a 30-year period. During the 1993 apparition, the early spring NPC appeared to be smaller than usual, with the cap's edge latitude being 3.7° smaller than the 1995 cap at 22° L_s. At the same time, there was a statistically significant increase in frequency of discrete localized and orographic clouds as well as in morning and evening limb clouds. These clouds appeared approximately 30° L_s earlier than expected. However, by late northern spring and early summer their frequency had dropped below that expected for the season. At the same time, the NPC demonstrated a fairly slow regression rate, being only 0.137°/°L_s, compared with 1995's 0.212°/°L_s for the same L_s period.

References: [1] James P. B. (1979) *JGR*, 84, 8332–8334. [2] Capen C. F. and Parker D. C. (1981) *J. Assoc. Lunar Planet. Observers*, 29, 38–41. [3] Parker D. C. et al. (1983) *Sky and Telescope*, 65, 218–220. [4] Beish J. D. and Parker D. C. (1988) *J. Assoc. Lunar Planet. Observers*, 32, 185–197. [5] Parker D. C. et al. (1990) *J. Assoc. Lunar Planet. Observers*, 34, 62–79. [6] Capen C. F. and Capen V. W. (1970) *Icarus*, 13, 100–108. [7] Foster J. et

al. (1986) *Earth, Moon, Planets*, 35, 223–235. [8] Beish J. D. and Parker D. C. (1990) *JGR*, 95, 14567–14675.

THERMAL INFRARED SPECTRA OF MARS OBTAINED IN 1988, 1990, AND 1993. T. L. Roush¹, G. C. Sloan², J. F. Bell III³, and C. W. Rowland⁴, ¹San Francisco State University, c/o NASA Ames Research Center, Mail Stop 245-3, Moffett Field CA 94035-1000, USA, ²NASA Ames Research Center, Mail Stop 245-6, Moffett Field CA 94035-1000, USA, ³Cornell University, Center for Radiophysics and Space Science, Space Science Building, Ithaca NY 14853-6801, USA, ⁴Stetson University and Wyoming Infrared Observatory, USA.

Thermal infrared spectral observations of Mars have been obtained during or near the past three martian oppositions [1–4]. The focus of these observations was to identify and characterize mineral salts (carbonates and sulfates) that are capable of sequestering atmospheric gases (CO₂ and SO₂) believed to have been released during Mars' earliest history but which are absent from the current volatile inventory [see 5]. If carbonates did form during some early epoch on Mars and have survived until the present, then these deposits would reflect where water was once abundant, such as ancient rivers, lakes, and/or oceans. Such deposits are likely locations for the evolution of life during Mars' earliest history, and would certainly represent prime targets for future missions to Mars.

Because the vibrational motions of atoms comprising these salts give rise to strong absorption of infrared radiation, infrared spectra of Mars provide a sensitive method of identifying these salts on the surface of Mars. Previous observations (1988) from the Kuiper Airborne Observatory (KAO) detected several features that were interpreted as being due to hydrates, carbonates, sulfates, and silicates [1], and subsequent thermal infrared observations from the KAO (1990), IRTF (1990), and WIRO (1993) [2–4] support this initial interpretation.

Knowledge concerning the identity and abundance of these volatile-bearing materials can provide valuable insight into the formation and evolution of the martian atmosphere. The global distribution of such materials can provide insight into both the spatial and temporal occurrence of liquid water on Mars. Knowledge regarding the relative abundance of surface hydrates would be invaluable for resource assessment for future missions to Mars. Data obtained at relatively high spatial resolution at IRTF (1990) and WIRO (1993) enable us to produce maps of the spatial distribution of the 10- μ m silicate opacity and can be used to address current sources and sinks of martian atmospheric dust.

While detailed analysis of the 1990 and 1993 observations are currently underway, the observations from the past three oppositions provide the capability to compare atmospheric dust opacity as a function of time. Such information is useful for assessing the interannual climatic variability on Mars. Here we derive the atmospheric dust opacity (τ) using the techniques described in detail by [1]. Briefly, (1) τ can be derived from spectral variations in the 8–9- μ m region because martian atmospheric CO₂ is relatively transparent at these wavelengths; (2) to facilitate our comparison from year to year we use the optical constants of montmorillonite 219b and the particle size distribution of [6]; (3) we use the radiative transfer formalism of [6,7] to calculate the flux from the martian surface at the viewing geometry appropriate to the observations;

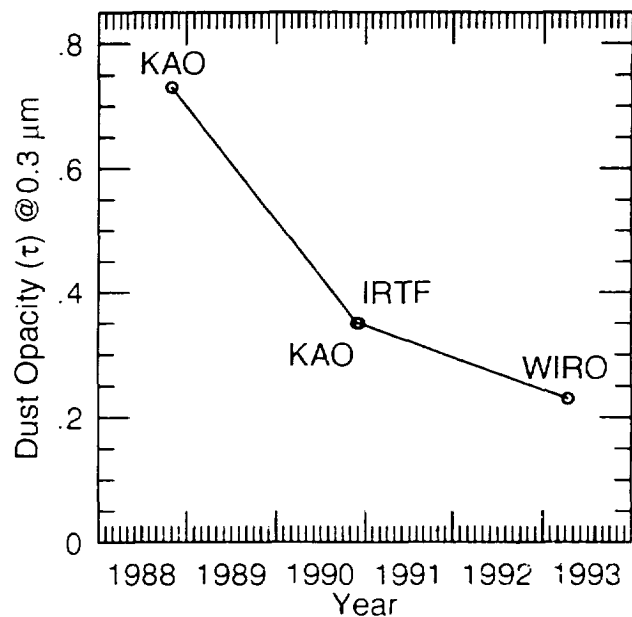


Fig. 1. Derived dust opacities from recent thermal infrared observations of Mars. For comparison purposes the models ignore atmospheric gases, use the particle size distribution of [7], and assume the dust is composed solely of montmorillonite clay [1,7].

(4) we calculate the brightness temperature (BT, the temperature of the blackbody required to produce the flux) from (3); and (5) we require the change in calculated BT to match the observational data.

The results for observations of regions located near the center of the martian disk, where the thermal contrast between the surface and atmosphere is the greatest, are listed in Table 1 and are shown graphically in Fig. 1. The dust opacity decreases by about 50% from 1988 to 1990 and by about 30% from 1990 to 1993. These results suggest a clearing of the atmosphere and are consistent with independent observations obtained in the microwave region [8,9] that also suggest a cold, clear martian atmosphere during recent oppositions.

TABLE 1. 1988–1993 thermal IR observations.

Year/ Platform	λ coverage (μ m)/ resolution	Detector array size	D_{eff} (")/ L_{p}	Aperture or pixel size	τ (0.3 μ m)
1988/KAO	5.5–10.5/60–100	24 \times 1	\approx 22/289	\approx 1/3 disk	0.73
1990/KAO	5.5–9.2/85–150	24 \times 1	\approx 18/340	\approx 1/4 disk	0.35
1990/IRTF	7.5–12.8/105–180	24 \times 1	\approx 18/345	\approx 1/20 disk	0.35
1993/WIRO	7.6–13.9/50–100	58 \times 62	\approx 9/47	\approx 1/20 disk	0.23

References: [1] Pollack et al. (1990) *JGR*, 95, 14595. [2] Roush et al. (1992) *LPS XXIII*, 1181. [3] Roush et al. (1991) *LPS XXII*, 1137. [4] Rowland et al. (1995) *LPS XXVI*, 1195. [5] Fanale et al. (1992) in *Mars* (H. Keiffer et al., eds.), 1135, Univ. of Arizona, Tucson. [6] Toon et al. (1977) *Icarus*, 30, 663. [7] Toon et al. (1989) *JGR*, 94, 16287. [8] Clancy et al. (1990) *JGR*, 95, 14543. [9] Clancy et al., *Bull. AAS*, 26, 1130.

SPECTROSCOPIC MEASUREMENTS OF ATMOSPHERIC WATER VAPOR. A. Sprague, D. Hunten, and R. Hill, Lunar and Planetary Laboratory, University of Arizona, Tucson AZ 85721, USA.

We have been fortunate with our synoptic observations of Mars during the 1994–1995 apparition and have obtained new water vapor measurements at eight additional L_s . Observations covering the end of northern winter through northern summer show a dramatic increase in water vapor abundance at high northern latitudes. The lowest abundance occurred at L_s 349 (late northern winter) with an average along the central meridian (218°) of only $1 \text{ pr } \mu\text{m}$. A peak value of $38 \text{ pr } \mu\text{m}$ was reached at L_s 107 (northern summer), at northern latitudes 50° – 70° . This value is typical of that measured by Viking under similar conditions [1]. It is also close to the record high values of up to $44 \text{ pr } \mu\text{m}$ seen by [2] in global averages from L_s 290–340 (southern summer). If, however, we were to average our values over all latitudes, our slit-averaged value would fall short of the Barker et al. maximum global value by a factor of 2. Nevertheless, this measurement illustrates the large interannual and latitudinal water vapor variations recorded since our systematic monitoring began in 1988 [3].

Our measurements are made with a high-resolution ($R \sim 180,000$) échelle spectrograph with a cooled CCD data acquisition system at the 1.5-m Catalina Observatory on Mt. Bigelow, Arizona (see Fig. 1 below). Because our equipment has a high quantum efficiency, and the chip is quite sensitive in the spectral region used (8177 – 8199 \AA), we can obtain high signal-to-noise spectral images with integration times of 10–15 min.

References: [1] Jakosky B. and Farmer B. (1982) *JGR*, 87, 2999–3019. [2] Barker E. et al. (1970) *Science*, 170, 1308–1310. [3] Rizk B. et al. (1988) *Icarus*, 90, 205–213.

MARS GLOBAL SURVEYOR CAMERA: CONTEXT OF EARTH-BASED OBSERVATIONS. P. Thomas, Center for Radiophysics and Space Research, Cornell University, Ithaca NY 14853, USA.

The Mars Global Surveyor Mission (MGS), partial replacement for Mars Observer, is to be launched to Mars in 1996 for a one-Mars-year survey mission. Among the instruments are cameras essentially identical to those flown on Mars Observer that will provide low-resolution global monitoring as well as very-high-resolution imaging of surface geology [1]. Both the low- and high-resolution images will address issues of martian climate and geology for which groundbased observations can provide crucial context information.

The wide-angle optics are line arrays supplying a 140° field of view that covers horizon to horizon plus 80 km off the limbs. Nadir resolution is 230 m/pixel . The single narrow-angle camera has a 0.44° field of view, or about 2.9 km wide at 1.4 m/pixel on the 2048 pixel line array. Images can be read out and stored with a variety of geometries and data compressions. Daily maps at 7.5 km/pixel will provide the basic monitoring database; seasonal maps at full resolution can be made.

The high-inclination, Sun-synchronous orbit makes this mission excellent for monitoring clouds, dust, surface albedo changes, and seasonal polar processes. The convergence of orbits near the pole means that the cap formation and recession can be monitored at full resolution. High-resolution images can be mosaicked near the polar extent of the orbit.

Polar dunes provide examples of the use of the MGS cameras in relation to Earth-based data. Dark dunes form a nearly continuous belt around the north polar layered deposits; in the south, dunes are concentrated locally in craters and other depressions. They may form a key marker of sediment types and movement into and out of

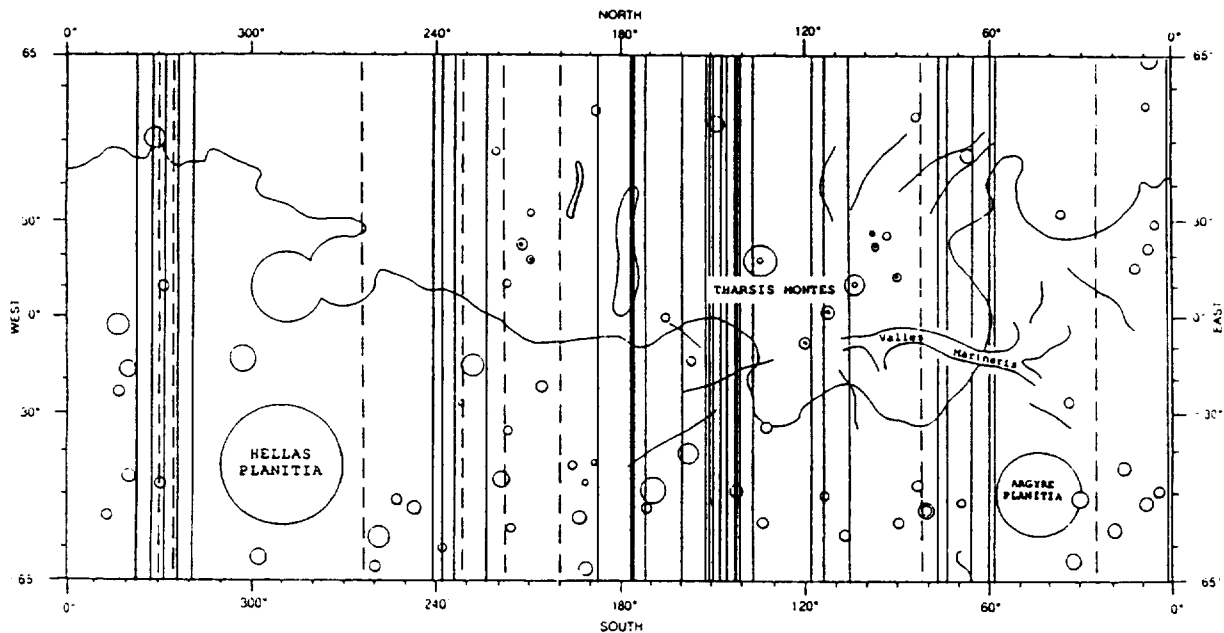


Fig. 1. A schematic representing Mars' surface with vertical lines placed at the longitudes of our water vapor measurements. Measurements were made at the 1.5-m Catalina Observatory with the LPL échelle spectrograph. Hatched lines are for the 1994–1995 apparition.

the layered deposits. They also may correlate with gaps in the seasonal polar cap observed by HST. MGS will be able to discern details of the dune morphologies (such as slipface size and smoothness) at many sites and provide information on their activity and the local effective winds. The wide-angle-camera data will allow mapping of frost recession characteristics in relation to underlying materials and topography, as well as mapping of wind transport of frost in parts of the fall and spring. These MGS data may provide the key to causes of cap recession variations visible in Earth-based data taken over many Mars years. Likewise, the timeline provided by Earth-based observations is then crucial in providing the temporal reference for the MGS data, as observations since Viking have shown changes in atmospheric clarity, temperature, and dust storm activity [2].

References: [1] Malin M. C. et al. (1992) *JGR*, 97, 7699–7718. [2] Clancy R. T. et al. (1995) *Icarus*, submitted.

THE 1992–1993 APPARITIONS OF MARS. D. M. Troiani, Mars Recorder, Association of Lunar and Planetary Observers, 629 Verona Court, Schaumburg IL 60193, USA.

During the 1992–1993 martian apparition, Mars was favorably placed high above the horizon, so despite its small apparent size it proved to be a very interesting planet for northern observers to watch. Mars presented us with many meteorological phenomena and a chance to investigate both the northern hemisphere of Mars and the northern polar cap (NPC). This was the first opportunity to view Mars' northern hemisphere since the 1983–1984 apparition.

With Mars so high in the sky most northern observers had, on average, fairly good seeing conditions (when it was clear) compared to a close apparition when Mars is more southerly. Unfortunately we had very unusual weather conditions worldwide, with many observers writing about the endless overcast nights. Consequently, the overall number of observations received might be low, but the quality of each observation was high.

An observer equipped with the right telescope and the proper color filters was able to track the progress of the many clouds that formed during this apparition. Color filters are the most important equipment needed by a planetary observer. They help overcome image deterioration caused by the Earth's atmosphere, permit separation of light from different levels in a planetary atmosphere, increase the contrast between areas of differing color, and reduce irradiation within the observer's eye. All these factors increase the sharpness of both surface and cloud details that are seen on Mars. Using color filters at the telescope can be a most challenging and rewarding experience, although weeks of practice may be necessary to condition oneself to detect those subtle wisps of clouds and hazes often observed in the martian atmosphere. Without the aid of these filters, many interesting phenomena may go undetected. These techniques will be useful during the next few apparitions of Mars.

Early white clouds, the appearance of orographic clouds around the large volcanos, and the reappearance of the Rima Tenuis earlier than predicted all point toward a warmer climate on Mars. This was first noticed by observers in the 1980s, so perhaps the warming trend on Mars is continuing.

North Polar Cap: We had a slightly rapid regress of the NPC during this apparition, as shown by meteorological phenomena like orographic clouds, bright limb haze, and the break-up of the north polar hood (NPH) all occurring earlier than predicted. Also we had

many observations of the reappearance of the Rima Tenuis starting in January.

Based on the results of the Oriental Astronomical Association (OAA) Mars Section and work done by A. Johnson, we now know that the NPC this year was about the same size as it was in 1979–1980. This year the NPC shrank at an average rate of around 7 km/day. Also, the NPC dark collar was distinct through at least early May ($L_s = 75^\circ$). It must be noted, though, that when the Rima Tenuis was first seen in all its glory in December 1979, it was observed as a notch and partial streak in the NPC.

G. Schiaparelli, using a 9" refractor in 1880, first noted that the NPC was divided in two parts by a dark rift. This observation was soon confirmed by Terby and Perrotin. This rift, then given the name "Rima Tenuis," was observed many times from 1901 through 1918. Recent records from the British Astronomical Association (BAA) show that the Rima Tenuis was possibly observed during 1933 and again in 1950. A search for it was carried out by the late C. Capen during the 1960s, which, despite using telescopes of 16", 30", and 82" in aperture, was unsuccessful. It was not until late 1979 that the Rima Tenuis appeared again, and it was a regular feature during the 1980 and 1982 apparitions.

The NPH was bright and large for most of this apparition until late November 1992. At this time the NPH started to slowly break up. When the NPC appeared it was brilliant and mostly clear afterward with a very dark collar around it. The NPC appeared at times to be "peanut" shaped with notches in the collar. Early CCD images by Don Parker showed a cold front moving off the NPC toward the south. As the NPH started to thin out in December we got views of some of Mars' far northern albedo features. Gerard Teichert of France was the first to see the NPC split into two parts by a rift on December 31 (not at the location of the Rima Tenuis). On January 18 I saw a notch in the NPC; by the 30th I could see a notch and a rift in it. Hernandez saw the NPC as "peanut" shaped on the 11th; on the 22nd Schmude observed a small bright spot on the NPC and a notch in it.

In January observers got a good view of the Rima Tenuis, the best since 1984. Rudolf Hillebrecht of Germany imaged it with a 6" telescope and a CCD camera. Jeff Beish, Carlos Hernandez, and I all saw it visually, and made some interesting drawings of it. The notch was again seen by Schmude in the NPC on February 3, 1993. The NPC appeared bright and whitish with an occasional local small cloud over it from January on. The south polar region was of interest because on many occasions a bright area near the southern limb was visible. Could this be the SPH (if it exists) or the beginnings of the development of the SPC?

Dust Activities: Mars presented us with a mostly clear atmosphere early in its apparition. This started to change in early October as observers saw a small dust cloud in the Chryse region. For the second apparition in a row we saw dust activity in this area. Again this past October, approximating what happened in 1990 (but on a smaller scale), Mars has shown us that very minor dust storms might be more common than we once thought. The 1990 (310° – $312^\circ L_s$) and the 1992 (335° – $342^\circ L_s$) storm events showed up without warning. They were very localized without any major changes in the martian albedo features. Major dust storms are rather rare events, and planetwide dust storms are very rare: only five have been reported in the history of Mars observations.

M. Minami of the OAA Japanese Mars Section first reported minor dust activity on Mars in early October. H. Ishadoh observed two minor dust streaks near Aurorae Sinus on October 3 ($334^\circ L_s$).

There was temporary darkening of Ganges and a slight fading of Nilokeras. Y. Higa was able to get videos of Mars showing the darkening of Ganges and the fading of the southern part of Nilokeras on October 2 (333° L_s). By October 6 an Ishadoh drawing showed that the Lunae Lacus again looks normal and Ganges a bit darker. Thus it looks as if the Japanese observers saw the beginning of some transient dust cloud activities on Mars. Observers viewed many dust streaks around the Chryse region throughout most of October. These dust clouds usually only lasted a few days.

In the U.S. several observers viewed some minor dust clouds in late October, again in the Chryse region. These streaks were very localized and fairly bright as observed in red light. Dan Joyce and Jim Carroll got a video of Mars with a black-and-white camera and a W#25 filter (red filter) on Dan's 20" telescope. The seeing was very bad, but after computer processing the image they noticed a bright cloud in Chryse on October 22, 1992 (344° L_s). An hour later on the same date, at 10:15 UT, under better seeing, I was able to observe a slightly bright streak in eastern Chryse extending into Xanthe. This cloud had a slight brightening toward its center. Aurorae Sinus appeared to have faded into a slightly shaded area as it might have been affected by this dust cloud. Sirenum Mare and Solis Lacus appear to be normal for this time of year.

A red filter is best for detecting martian dust clouds. For example, the Chryse region usually appears slightly bright in any case, and a filter brings out the details in these types of dust streaks. Martian dust clouds are reddish in appearance, so with a red filter they remain bright.

In early November all the dust activity settled down, and the atmosphere returned to its normal clarity until December, when we started to see an increase in white clouds. We had no martian dust clouds or storms of any good size that were visible from November to April. We did have a small disturbance or dust cloud move over Sabaeus Sinus and Meridianii Sinus in early May as reported by Rhea.

Meteorological Activity: Mars meteorological activity began in late November as the NPH started to slowly break up. The first observation of this was my view of Mars in late November, when I saw numerous high thin white clouds visible in violet light (W#47) in the northern hemisphere and around the NPH. Thus began a series of moderate white cloud activities with considerable bright morning and evening limb haze. Some appeared bright even in red light, apparently because of some fine dust in the cirrus white clouds. Orographic clouds were observed near the large volcanos such as Olympus Mons and in the Tharsis region. These clouds appeared a full month earlier than predicted. This was another indication that the NPC retreated rapidly. These discrete white orographic clouds are seen in martian spring and summer forming on the upper slopes of the large volcanos. Mariner and Viking spacecraft identified them as water clouds. Also, we had some evidence of equatorial cloud bands (ECBs). These ECBs were visible across the Tharsis region extending into Amazonis. ECBs are a faint veil of wispy white clouds that vary in shape and transparency that extend across the martian equatorial region. These ECBs are best detected in violet light and reside at a chilly high altitude and are probably composed of CO₂ ice crystals. There were some "blue clearings" reported at times. There were white clouds observed over Libya, Argyre I, Arabia, Memnonia, Electris, Noachis-Serpentis, Eridania, and Ausonia. Fog was seen in Hellas on many occasions.

All this meteorological activity is typical of this martian season,

although some occurred a little early. It must be remembered that in order to make useful observations of the martian atmosphere a set of photovisual color filters is highly desirable. Color filters help overcome image deterioration and permit separation of light from different levels in the planetary atmosphere, thus aiding the exploration of different depths and cloud levels in the martian sky.

In early December the NPH started to thin out. On December 5, Don Parker showed an NPH thinning with some rifts in it. The next day albedo features were seen through the NPH. The Hellas region was bright with fog in early December. By the 20th white clouds were over the NPC, and in violet light I observed high clouds near the NPC. The very next day, Parker got CCD images of orographic clouds over the Tharsis volcanos and around Olympus Mons. (These were also seen by Rhea, Melillo, and me). In addition, the crater Newton was noted as a black dot just south of Atlantis I in Electris (Parker CCD). A very dark notch was seen in the NPC with a bright cloud over it on December 25 (Rhea). Johan Warell of Sweden observed a white area near Syrtis Major with fog again in Hellas. Most of late December and through all of January, some very bright evening and morning limb haze was discerned. Hernandez (December 22) saw the NPC with an indentation north of Propontis I (at 170°W) corresponding to Devalidianus and a north polar cloud adjacent to the NPC over Terne. The last important observation of 1992 was by Gerard Teichert (France) who saw the NPC split into two patches by a rift. In December we received numerous reports of a very good "blue clearing" as seen in violet light (W#47). Murakami, of the OAA, watched the relation of M. Acidaliu with the NPR in mid December. Some bright matter split off from what was left of the NPH only to cover an area of M. Acidaliu with a white haze.

January 7 marked the martian opposition and a month of outstanding observations commenced. The Chryse-Xanthe region was very bright, covered by a haze as seen in blue light. We had a bright cloud near Temple. The NPC had signs of activity with bright clouds on or near it. At times, the NPC was noted to be "peanut" shaped (Hernandez). A cloud was again seen over Olympus Mons, this time by Heath of the BAA. A very bright small circular cloud was seen over the Libya Basin and again fog was detected in the Hellas Basin. The English observer McKim saw a bright white cloud over Argyre I. Both the evening and morning limbs had bright clouds adjacent to them from time to time. Insula was obscured by a semicircular bright patch, possibly fog or a cloud in or over the crater Huygens. There was a white haze visible along the southern limb that started in January and continued for months. This bright area could be related to the SPC, which itself was not visible. This cloud mass was highly variable in intensity and not seen on all nights.

There was an abundance of cloud activity on Mars again during February. McKim saw the Hellas region bright, with bright patches in northwest Hellas, as well as Libya. Heath (BAA) saw the Libya cloud cross over the Syrtis Major region. We had reports of bright clouds in the Noachis-Serpentis region, Hellas, Libya, hints of the SPH, Zephyria, Electris, and a very large and bright white cloud over Eridania extending into Ausonia (Troiani). This cloud activity was reported by Robinson, Melillo, Rhea, McKim, Fabian, Heath, Warell, and Troiani. The ECB was seen by Rhea. There was a white cloud in the vicinity of Arabia. It was noted also in February that the NPC was shrinking rapidly.

By March there was still a cloud visible in both Memnonia and Electris. There was a cloud in Ganges and again Libya was very bright. Bright equatorial clouds and cloud activity around Argyre

were seen by Rhea. These ECBs were seen by Johnson (BAA) at 63° longitude. There was also some cloud activity in the Lunae Lacus vicinity. In early May there was a bright cloud covering parts of Syrtis Major. We had a bright spot in Iadylgia, and the SPR was very bright white. Clouds were seen in the Ausonia-Australis region, and a bright spot appeared to be in Libya. Hellas was bright with fog.

As Mars continued to recede in June the number of observations diminished. We have had a few good observations that reveal bright clouds in the Amazonis and Tritonis Sinus regions. Proponis was seen as a small dark rod. We had a number of observations demonstrating that there were clouds again visible over the Tharsis region and, of course, over the great volcano Olympus Mons. Bright limb haze continued to form on numerous occasions over both the evening and morning limbs throughout the latter half of this apparition.

The Future: The 1992–1993 apparition of Mars proved to be a very exciting observing season with always something of interest on the Red Planet. This apparition has convincingly revealed that a very close approach of Mars is not essential to find things of interest. Thus, despite being near aphelic, the next three oppositions of Mars (1995, 1997, and 1999) will have the northern hemisphere and the NPC tilted toward Earth and the Sun. These coming apparitions will have as much interesting meteorological activity as we just had in 1992–93.

Acknowledgments: Members of the Association of Lunar and Planetary Observers, the British Astronomical Association, and the Oriental Astronomical Association contributed to this article. Their efforts are gratefully acknowledged.

1994–1995 APPARITION OF MARS. D. M. Troiani, Mars Recorder, Association of Lunar and Planetary Observers, 629 Verona Court, Schaumburg IL 60193, USA.

The 1994–1995 apparition of Mars was an aphelic opposition, making it the poorest (in apparent size) in over a decade. When Mars reached opposition in early February it had an apparent size of only 13.9 arcsec; however, for the serious Mars observer, this apparition turned out to be very exciting because it was high in the sky for northern observers and provided views of the increasing meteorological activity on the planet. Most of the research of the Association of Lunar and Planetary Observers' International Mars Patrol (IMP) was concentrated on martian meteorology and north polar cap (NPC) behavior. Their observational programs for this apparition are discussed here.

Introduction: The 1994–1995 apparition was very exciting for all observers despite Mars' small apparent size. There were many interesting rifts and weblike features crossing all over the NPC. Limb clouds were always present in the morning and/or evening and a variety of local clouds covered the Tharsis region and other areas. There was a very active cloud formation in the martian atmosphere, which was rich in water vapor from the NPC. Throughout this apparition we had reports of numerous cloud features such as orographic clouds, equatorial band clouds, and the "Syrtis blue cloud." We received over 2250 observations from IMP observers all over the world, an impressive number considering it was an aphelic apparition and Mars was over 100 million km away from Earth at its closest approach. We received over 400 measurements of the NPC areocentric latitude that were obtained between 22° and 122° L_s from bifilar micrometer, CCD, and video red-light images. Some

interesting relationships between Mars meteorology and NPC behavior appear to be emerging.

North Polar Cap: From June to late October the north polar hood (NPH) was bright and visible, followed by a period when it was fragmented, with the NPC partially visible. After that the NPH was mostly clear, with a dark collar, which first appeared in mid October, around the NPC. At times, high thin clouds were visible in blue light over the NPC. An Arctic cold front pushed clouds toward the south of the NPC on the morning limb on October 7, 1994, and again on November 3. From October through November 1994 a slight haze was seen over the NPC when observed in blue light.

Observations made during the months of December and January have provided very strong evidence that the Rima Tenuis and the Rima Borealis are back. Giovanni Schiaparelli, who gained fame by using the term "canali" to describe threadlike patterns across the martian terrain, first detected the "Rima Tenuis" in 1888, giving it this name because it appeared to be a very faint rift running through the fluctuating cap. This is the fifth aphelic apparition in a row in which the Rima Tenuis has been observed. During this apparition it looked different than it did during past apparitions, which could be due to Mars' north polar region having an especially accentuated tilt toward Earth. Observations of the Rima Tenuis have been difficult. In CCD images it has appeared to be wide and diffuse at the edges, while to the visual observer it appears as very thin lines starting at a very small notch at 332° longitude.

In January both Hiroshi Ishadoh of the Oriental Astronomical Association (OAA) Mars Section (Japan) and Don Parker observed a shadowy streak in the NPC that Masatsugu Minami of the OAA believes to be the early start of the Rima Borealis. It appears that we now have enough observations to conclude that we are seeing both the thin rift of the Rima Tenuis and the larger, diffuse Rima Borealis. To date we have 24 visual and 17 CCD images from 16 observers from around the world.

Unknown to us at the time, the first sign of something unusual was in Don Parker's CCD images in late October and November. They reveal that the NPC had a very faint dark diffuse thin rift cutting the cap lengthwise. D. Niechoy of Germany saw a rift of some kind in the cap on December 2. Next, Samuel R. Whitby saw a notch in the NPC at 80° on December 20, and also observed the NPC cut in half on December 21, 1994, by a large, diffuse rift of some kind. Then on December 26, 1994, three observers from the Midwest saw something in the cap.

I first detected Rima Tenuis as a notch in the martian NPC at 332° at 05:05 UT on 12/26/94 with a 17.5" f/4.5 telescope at my observatory (The Rima Tenuis Observatory) using 317× with a red filter (W#25). Seeing conditions were a 9.5 (1–10, 10 best). The notch was confirmed by an observation made by Gary Cameron (Ames, Iowa) at 06:40 UT also on December 26. He also observed it as a dusky notch with half of the NPC being brighter than the rest. After heavy processing, CCD images observed by Mark Schmidt using a W#23A filter, also on December 26, at 07:21 UT, showed both the notch and the rift cutting across the NPC. On December 31, 1994, during a cap measurement procedure, Don Parker, using his 16" f/6 telescope at his home in Coral Gables, Florida, observed the whole rift cutting across the NPC. He made both a visual drawing and CCD images in red light (W#25).

From the Parker cap measurement it appears that the NPC is slightly smaller than normal for this time of season (L_s). These observations of this small cap size support the idea that Mars is

going through a slightly warmer period that started in late December 1979 when the Rima Tenuis first appeared after not being seen in over 60 years. Parker got CCD images of both rifts on December 23, 25, 26, 27, 30, 31, January 1, 2, and 4. His best images were obtained on December 31, when the Rima Tenuis was very dark and large. One of our younger observers, Ted Stryk from Bristol, Virginia, using his 10" f/4.5 telescope, made some wonderful drawings of it at the beginning of January.

The next observations of this rift were reported on January 26 at 02:50 UT by both Dan Joyce and me using the Cernan Space Center (Triton College) 10" f/8 reflector telescope. I got a drawing showing the complete rift with my 17.5" f/4.5 telescope the next day, January 27, 1995. Mark Schmidt and Chris Tobias obtained CCD images at the Racine Observatory (Wisconsin) on January 27, 1995, that clearly show the Rima Tenuis notch in the south edge of the NPC. Later that same night (9:30 UT), Joyce observed many small fine rifts in the cap using his own 10" telescope.

On January 29 a number of observers from the Midwest region observed the Rima Tenuis. Joyce, with his 20" f/4.5, saw the very small notch and the rift at 04:30 UT. I saw it at the same time with my 17.5" telescope. The rift was very thin but dark, making it easily visible at times of fine seeing. Two other local observers got a view of it. Darren Drake glimpsed it with his 17.5" telescope; although it was hard to see it was still visible. In Chicago, Jesse Carroll saw the rift plainly with his 6" f/10 Newtonian. On January 30th, Mark Schmidt got the best CCD images of the Rima Tenuis starting at the small notch in the NPC at 332° longitude and cutting across the cap. Images from the HST shown a faint streak in the cap at the right longitude. So it appears that this rift is real! The next images of this rift were on CCD images by Don Parker in May 1995.

Meteorological Activities: Clouds, clouds, and more clouds is what many observers reported on Mars from January through March 1995. We had an abundance of morning and evening limb cloud activity, with some clouds being very bright at times. Don Parker and Jeff Beish first reported the "Syrtis blue cloud" on January 28. This is a very localized cloud that has been traced for over a century. It recurs every martian year around the northern hemisphere summer solstice and then persists through most of early summer. This cloud circulates around the Libya Basin and then crosses over to the Syrtis Major region. It then changes the color of this albedo feature to an intense blue. Chick Capen named this feature the "Syrtis blue cloud" because when viewed through a yellow filter the Syrtis Major turned a vivid "green." This type of cloud was first observed by Angelo Secchi of the Vatican Observatory in 1858. The cloud was next seen by J. N. Lockyear in 1862 and again in 1911 by members of the British Astronomical Association (BAA). C. W. Tombaugh and Capen saw the cloud early in the martian northern hemisphere summer during the apparition of 1950. It was seen regularly in the 1960s and it was most prominent in 1982. Jeff Beish also reported on February 18 a cloud formation over Xanthe-Memnonia that he calls the "Capen wedge cloud."

There was some evidence of equatorial cloud bands during February. By the 28th, Parker's CCD images showed fairly bright equatorial cloud bands. There were persistent clouds over Libya, next to Syrtis Major, from January 28 to about February 24. On February 8, T. Cave saw a bright cloud projection at the evening limb that lasted for 40 minutes. Orographic clouds, like those that form on Earth, are white discrete clouds that are condensed from the moisture-laden air that is uplifted over a mountain or volcano, and

were over Olympus Mons on February 18. Orographic clouds, which form when the martian atmosphere is high in water vapor especially in late spring or early summer of the northern hemisphere, appear bright on Mars when viewed through a blue (W#80A) or a violet (W#47) color filter.

There was a large "W cloud" (an orographic cloud over the Tharsis region) on the evening limb on the 19th. When these discrete cloud dots grow so large that they coalesce to form the characteristic letter "W," the famed W cloud becomes apparent. In late February there also were discrete clouds over Xanthe, Amazonis, Argyre I, and Arabia-Moab. CCD images by Parker showed on the 20th two sets of equatorial band clouds crossing over both the Amazonis and the Tharsis regions. On the 24th Cameron saw a small bright spot in the Solis Lacus region and clouds over Tharsis. Hellas had some light fog in early March. The Elysium region had a bright cloud over it on March 15 and the Eridania was bright. On March 16 there were a few very small bright spots in Cebrenia and Utopia.

The NPC was again very interesting to observe because, when seeing conditions were very good, great amounts of faint details were visible in it. The south edge of the NPC was seen to be irregular in shape at times. There were many reports of rifts (including the Rima Tenuis) in the cap. Recent images of Mars from the HST clearly show the Rima Tenuis rift in the NPC. Dan Joyce observed on February 12 and on other dates in February that the NPC appeared to him to be smoky. At the Winter Star Party at least 10 observers asked me about the rifts and other unusual things they had been seeing in the NPC. Jeff Beish saw a light haze over the cap, possibly the start of the "aphelic chill" on February 8. This occurs in late spring as a hood that suddenly appears over the north cap. It is most likely caused by a sudden outlet of water vapor that condenses over the frigid polar region.

Dust Activities: As was expected, no major dust clouds were visible during this period, but we did observe some very minor dust activity. On October 5 it appeared that there was dust in the atmosphere over Chryse, at times making it very bright in red light. Also there was a small thin dust cloud in Xanthe that was first observed by Whitby on November 3. It was seen again by Ted Stryk on November 13 and 14. On November 14 it seemed to him that it had grown since the day before. There was some dust mix in the clouds over the Chryse region in March and a small dusty spot near Solis Lacus. This was apparently the extent of dust activity during the 1994-1995 apparition.

Can Amateur Observations Still Be Worthwhile? The answer is definitely YES!! The Mars Section assisted several professional planetary scientists during the recent apparition by responding to requests for ALPO Mars data. One request came from Fred Espenak of the NASA Goddard Space Flight Center's Planetary Systems Branch. He observed Mars in March 1995 in the 10- μ m spectroscopic range with NASA's 3-m telescope (IRTF) on Mauna Kea. He was measuring the distribution of ozone in Mars' atmosphere using Goddard's IR heterodyne spectrometer. In his analysis of these data he needed to know the transparency of the martian atmosphere at the time of his observation. Our data showed him what clouds or haze activity were present before, during, and after his observing run on Mauna Kea.

All the Mars recorders were invited to present papers at the Mars Telescopic Observations Workshop convened by Jim Bell and Jeff Moersch of the NASA Planetary Astronomy Program at Cornell University and sponsored by the Lunar and Planetary Institute. The

theme of this workshop was to explore the role that current and continuing Earth-based observations can play in increasing our understanding of Mars. It brought together professional and amateur astronomers who observe at different wavelengths and don't often have the opportunity to share their ideas. Don Parker gave a talk on his "Mars Watch" program, which involves telescopic observations of Mars using a variety of special filters. Dan Joyce presented my ALPO Mars Section results from both the 1992–1993 and the 1994–1995 martian apparitions.

The papers by amateur astronomers were all well received and generated a great deal of interest from the professional astronomers who attended this workshop.

For More Information: The ALPO Mars database and computer maps are available to all interested astronomers. Maps are produced by ALPO Mars Recorder Dan Troiani. If you need any data for the past two apparitions, or if you would like more information on the ALPO Mars Section, contact the author at the address listed above, or phone 708-529-1716.

Acknowledgments: The Mars Section of the Association of Lunar and Planetary Observers wishes to express its gratitude for the contributions of fellow ALPO members as well as those of the British Astronomical Association and the Oriental Astronomical Association.

PROSPECTS FOR OBSERVING MARS FROM ANTARCTICA DURING THE UPCOMING OPPOSITIONS OF 1999, 2001, AND 2003.

F. R. West, 520 Diller Road, Hanover, PA 17331-4805, USA.

Introduction: Calculations of the physical parameters for observing Mars from Antarctica have been made for its future oppositions of 1997, 1999, 2001, 2003, and 2005 [1].

This paper continues this research. It uses the precise ephemeris for Mars found in [2] to find the physical parameters for observing Mars from Antarctica. Comparison with [1] showed approximate agreement for most values that I calculated earlier. The unfavorable opposition of 1997, which I considered using for test observations at possible observing sites, was not considered here; such observations will be made at the start of the 1999 observing season. The unfavorable opposition of 2005 also was not considered here [see 1]. The improved physical parameters found here for observing Mars have been used to evaluate prospects for the continuous observation of Mars from the Amundsen-Scott station at the South Pole (90°S latitude) during the oppositions of 1999, 2001, and 2003.

Procedure and Results: The observing season is assumed to last from April 11 to September 2 in the Antarctic autumn and winter, when the Sun's altitude is $< -8^\circ$ and far enough below the horizon to make the sky dark enough to observe. The physical parameters for observing Mars found here are shown in Table 1 for the 1999, 2001, and 2003 oppositions. Selected dates are listed in column 1; for those dates, the altitude h_{\oplus} of Mars at the South Pole is shown in column 2, its apparent diameter d_{\oplus} is shown in column 3, and the seasonal longitude of Mars L_s is shown in column 4.

Results for the 1999 Opposition: Mars is never higher than 21.67° above the horizon during this observing season. It is 12.9° above the horizon when the observing season begins, but its altitude

has decreased to $h_{\oplus} = 11.7^\circ$ by opposition on April 24, when Mars has the apparent diameter $d_{\oplus} = 16.0$ s. Mars' minimum altitude $h_{\oplus} = 9.67^\circ$ occurs on May 28, when $d_{\oplus} = 14.7$ min, after which its altitude increases steadily to $h_{\oplus} = 21.67^\circ$ at the end of the observing season, when $d_{\oplus} = 7.9$ min and $L_s = 198^\circ$. The martian seasons for this observing season are from midsummer to early autumn in the northern hemisphere and from midwinter to early spring in the southern hemisphere. Since this opposition is not as favorable for observing Mars from Antarctica as are the next two oppositions, part of the observing time may be used to test sites, telescopes, and equipment for later observations. However, possibilities will exist at this opposition to observe Mars' residual water-ice north polar cap, possibly the formation of the north polar cap. This observing season also includes the start of the so-called "dust storm season" on Mars ($L_s \approx 160^\circ$; see [3]) on June 25, when $d_{\oplus} = 12.0$ min.

Results for the 2001 Opposition: This is by far the best opposition for observing Mars from Antarctica. Mars has an altitude $h_{\oplus} > 23^\circ$ at the South Pole for the entire observing season, and will be above the horizon continuously for almost all of Antarctica. Weather permitting, this will make possible continuous observation of Mars for $144^\circ \leq L_s \leq 225^\circ$, corresponding to martian northern hemisphere late summer to mid autumn and southern hemisphere late winter to mid spring. This makes it possible to study changes in both seasonal polar caps as well as any polar hoods. The north polar region is slightly more favorably placed for observation than the south polar region for most of the observing season. The "dust storm season" begins May 12, when $d_{\oplus} = 16.2$ s, and continues for the rest of the observing season. Mars will be at opposition June 13 and will appear largest ($d_{\oplus} = 20.8$ s) on June 21.

Results for the 2003 Opposition: At opposition on August 28, 2003, Mars will be closer to the Earth than it has been since 1719; its apparent diameter will then be 25.1 s. However, $h_{\oplus} = 15.7^\circ$ then, which is considerably lower than its altitude at the South Pole was during the entire 2001 observing season. Nevertheless, the 2003 observing season will be fairly good for observing Mars from Antarctica; $166^\circ \leq L_s \leq 253^\circ$ for it, corresponding mainly to northern hemisphere autumn and southern hemisphere spring. Unlike the 1999 and 2001 oppositions, Mars' southern hemisphere and polar cap will be better placed for observation than the northern ones will be. Polar studies, cloud, and especially dust storm monitoring should have priority at this opposition.

Conclusions: (1) Efforts should be made to observe Mars as continuously as possible from Antarctica during the 1999, 2001, and 2003 oppositions. At least one dedicated 30–60-cm aperture Cassegrain telescope with proper instrumentation (a CCD camera with suitable filters and an infrared spectrometer) should be installed at an Antarctic site(s) exclusively for the observation of Mars during these oppositions. (2) Telescopes dedicated to continuous monitoring of Mars should be fully automated if possible. (3) Antarctic sites other than the South Pole, especially those on the high Antarctic Plateau, such as Dome A (82° S latitude, 85° E longitude), should be investigated for mostly clear skies, calm air, and good transparency and seeing for possible installation of more telescopes to monitor Mars [see 1,4].

References: [1] West F. R. (1994) *Bull. AAS*, 26, 1117–1118. [2] Espenak F. (1994) *NASA RP-1349*, 135–144. [3] Martin L. J. and Zurek R. W. (1993) *JGR*, 98, 3221–3246. [4] Sweitzer J. S. (1993) *Mercury*, 22, 13–18.

TABLE 1. Physical parameters for observations of Mars from the South Pole, Antarctica (90°S latitude).

Date	Altitude of Mars h_M (°)	Apparent Diam. of Mars, d_M (arcsec)	Seasonal Long. Mars L_s (°)
<i>1991 Opposition</i>			
Apr. 11	12.9	15.1	122.5
Apr. 24	11.7	16.0	129 *
May 1	11.0	16.2	132 †
May 28	9.7	14.7	145
July 1	12.0	11.5	163
Aug. 1	16.56	9.4	180
Sept. 1	21.65	7.9	198
<i>2001 Opposition</i>			
Apr. 11	23.27	11.5	143.9
May 1	24.15	14.3	154.1
May 23	25.35	17.9	165.8
June 13	26.5	20.6	177.9 *
June 21	26.72	20.8	182.4 †
July 4	26.86	20.3	189.3
July 30	26.86	17.3	204.6
Aug. 25	27.02	14.1	220.5
Sept. 2	26.99	13.2	225.5
<i>2003 Opposition</i>			
Apr. 11	22.3	8.1	166.3
May 1	20.4	9.5	177.3
May 21	17.96	11.2	188.7
June 10	15.53	13.5	200.4
June 30	13.67	16.5	212.5
July 20	13.04	20.1	224.9
Aug. 9	14.04	23.7	237.5
Aug. 19	14.95	24.8	243.8
Aug. 27	15.68	25.1	249 †
Aug. 28	15.76	25.1	249.8 *
Sept. 2	16.11	25.1	252.7

* Mars is at opposition.

† Mars is closest to Earth.

List of Workshop Participants

Tokuhide Akabane

*Hida Observatory
Kyoto University
Kamitakara, Gifu 506-13
JAPAN
Phone: 81-578-6-2311
Fax: 81-578-6-2311
E-mail: akabane@kusastro.kyoto-u.ac.jp*

Sushil K. Atreya

*Department of Atmospheric and Oceanic Studies
2210 Space Research Building
University of Michigan
Ann Arbor MI 48109-2143
Phone: 313-763-6234
Fax: 313-764-5137
E-mail: atreya@umich.edu*

Ed S. Barker

*Code SL
NASA Headquarters
Washington DC 20546
Phone: 202-358-0289
Fax: 202-358-3097
E-mail: ebarker@sl.ms.ossa.hq.nasa.gov*

James Bell

*Center for Radiophysics and Space Research
424 Space Sciences Building
Cornell University
Ithaca NY 14853-6801
Phone: 607-255-5911
Fax: 607-255-9002
E-mail: jimbo@marswatch.tn.cornell.edu*

David Crisp

*Mail Stop 169-237
Jet Propulsion Laboratory
4800 Oak Grove Drive
Pasadena CA 91109
Phone: 818-354-2224
Fax: 818-393-0071
E-mail: dc@crispy.jpl.nasa.gov*

Michael Disanti

*Code 693
NASA Goddard Space Flight Center
Greenbelt MD 20771
Phone: 301-286-7036
Fax: 301-286-1629
E-mail: ysmads@lepvax.gsfc.nasa.gov*

Kenneth S. Edgett

*Department of Geology
Box 871404
Arizona State University
Tempe AZ 85287-1404
Phone: 602-965-0204
Fax: 602-965-1787
E-mail: edgett@esther.la.asu.edu*

Ian E. Harris

*RASC-Montreal
536 Crescent St. Lambert
Quebec
CANADA
Phone: 514-671-7339
Fax: 514-671-8518*

Joe Havrilla

*P.O. Box 664
Croton-on-Hudson NY 10520
Phone: 212-499-4635*

Ken Herkenhoff

*Mail Stop 183-501
Jet Propulsion Laboratory
4800 Oak Grove Drive
Pasadena CA 91109-8099
Phone: 818-354-3539
Fax: 818-354-0966
E-mail: Ken.E.Herkenhoff@jpl.nasa.gov*

Jeffrey L. Hollingsworth

*NRC Research Associate
Mail Stop 245-3
NASA Ames Research Center
Moffett Field CA 94035
Phone: 415-604-6275
Fax: 415-604-6779
E-mail: jeffh@humbabe.arc.nasa.gov*

Don Hunten

*Lunar and Planetary Laboratory
Department of Planetary Sciences
University of Arizona
Tucson AZ 85721
Phone: 520-621-4002
Fax: 520-621-4933
E-mail: dhunten@lpl.arizona.edu*

Philip James

*Department of Physics and Astronomy
University of Toledo
Toledo OH 43606
Phone: 419-530-4906
Fax: 419-530-2723
E-mail: pj@physics.utoledo.edu*

Daniel Joyce

*ALPO Mars Section
12911 Lerida St.
Coral Gables FL 33156
Phone: 305-665-1438*

David R. Klassen

*University of Wyoming
Box 3905, University Station
Laramie WY 82071
Phone: 307-742-3945
Fax: 307-766-2652
E-mail: drk@uwyo.edu*

Vladimir A. Krasnopolsky

*Code 693
NASA Goddard Space Flight Center
Greenbelt MD 20771
Phone: 301-286-1549
Fax: 301-286-1683
E-mail: ys2vk@lepvax.gsfc.nasa.gov*

Steve W. Lee

*Laboratory for Atmospheric and Space Physics
Campus Box 392
University of Colorado
Boulder CO 80309
Phone: 303-492-5348
Fax: 303-492-6946
E-mail: lee@syrtris.colorado.edu*

Leonard Martin

*Lowell Observatory
1400 Mars Hill Road
Flagstaff AZ 86001
Phone: 520-774-3358
Fax: 520-774-6296
E-mail: ljm@lowell.edu*

Jeffrey E. Moersch

*427 Space Sciences Building
Cornell University
Ithaca NY 14853
Phone: 607-255-4709
Fax: 607-255-5907
E-mail: moersch@astrosun.tn.cornell.edu*

Didier Moreau

*Belgian Institute for Space Astronomy
Avenue Circulaire 3
Brussels B1180
BELGIUM
Phone: 32-2-373-0367
Fax: 32-2-374-8423
E-mail: moreau@hermes.oma.be*

Christian Muller

*Belgium Institute for Space Astronomy
Avenue Circulaire 3
Brussels B1180
BELGIUM
Phone: 32-2-374-2728
Fax: 32-2-374-8423
E-mail: chris@hermes.oma.be*

Donald Parker

*ALPO Mars Section
12911 Lerida St.
Coral Gables FL 33156
Phone: 305-665-1438*

Ted L. Roush

*Mail Stop 245-3
Space Science Division
NASA Ames Research Center
Moffett Field CA 94035-1000
Phone: 415-604-3526
Fax: 415-604-6779
E-mail: roush@barsoom.arc.nasa.gov*

Martha W. Schaefer

*Department of Geology and Geophysics
P.O. Box 208109
Yale University
New Haven CT 06520-8109
Phone: 203-432-3116
Fax: 203-432-3134
E-mail: schaefer@syrtris.geology.yale.edu*

Ann L. Sprague

*Lunar and Planetary Laboratory
Room 325, Space Science Building
University of Arizona
Tucson AZ 85721
Phone: 520-621-2282
Fax: 520-621-4933
E-mail: sprague@lpl.arizona.edu*

Steve Squyres

*Space Sciences Building
Cornell University
Ithaca NY14853
Phone: 607-255-3508
Fax: 607-255-5907
E-mail: squyres@astrosun.tn.cornell.edu*

Peter Thomas

*422 Space Sciences Building
Cornell University
Ithaca NY 14853
Phone: 607-255-5908
Fax: 607-255-9002
E-mail: thomas@cuspid.tn-cornell.edu*

Jeff Van Cleve

*Space Sciences Building
Cornell University
Ithaca NY 14853-6801
Phone: 607-255-5901
Fax: 607-255-5875
E-mail: vanclave@astrosun.tn.cornell.edu*

Frederick R. West

*520 Diller Road
Hanover PA 17331-4805
Phone: 717-632-6055*

